

COMPOSITE OPEN-WEB TRUSSES WITH
METAL CELLULAR FLOOR

COMPOSITE OPEN-WEB TRUSSES WITH
METAL CELLULAR FLOOR

by

MOKHTAR HAMED AZMI, B.Sc. Eng.

A Thesis

Submitted to the Faculty of Graduate Studies
in Partial Fulfilment of the Requirements
for the Degree of
Master of Engineering

McMaster University

April 1972

MASTER OF ENGINEERING (1972)
(Civil Engineering)

McMASTER UNIVERSITY
Hamilton, Ontario,
Canada.

TITLE: Composite Open-Web Trusses with Metal Cellular Floor

AUTHOR: M.H. Azmi, B.Sc. Eng. (Ain Shams University, Cairo)

SUPERVISOR: Dr. H. Robinson

NUMBER OF PAGES: xiii, 95

SCOPE AND CONTENTS:

This thesis involves the testing and analysis of six, 50 ft. span open-web joists. A design procedure for this type of construction is proposed.

ACKNOWLEDGEMENTS

I wish to thank my supervisor, Dr. H. Robinson for his valuable guidance throughout the course of this work. I am also grateful to the Civil Engineering Department, McMaster University for providing the teaching assistantship and to the members of the staff for their helpful suggestions and encouragement.

The investigation was supported by a grant from the Canadian Steel Industries Construction Council. The trusses were provided by Anthe's Steel Products Ltd., York Steel Construction Ltd. and Great West Steel Industries Ltd., and the metal floor by Robertson-Irwin Ltd. The stud shear connectors were supplied and fitted by Nelson Stud Welding, Ltd.

I also wish to thank the technicians of the Applied Dynamics Laboratory for their assistance, Miss Carlene Pepper for typing the manuscript and Mr. U. Golts for taking the photographs. Special thanks to my wife for her patience throughout the past year.

ABSTRACT

Tests on six composite open-web steel joists and concrete slabs with ribbed metal decking are described.

The joists spanned 50 ft. and were loaded by two symmetrical point loads.

Different types of shear connectors and different degrees of connection were used.

Tests results are shown and compared with analytical results obtained from elastic theories.

An ultimate strength design method is proposed.

TABLE OF CONTENTS

Title Page	i
Scope and Contents	ii
Acknowledgements	iii
Abstract	iv
Table of Contents	v
List of Tables	vii
List of Figures	viii
Notations	x
CHAPTER I - INTRODUCTION	1
1.1 Composite Beams	1
1.2 Previous Research	2
1.3 Advantages and Economics of the System	6
1.4 Object of Research	8
CHAPTER II - DESCRIPTION OF TESTS	11
2.1 Test Specimens	
2.2 Testing Procedure	15
CHAPTER III - TEST RESULTS	19
3.1 Anthes Joists	19
3.1.1 Beam (I)	19
3.1.2 Beam (II)	24

3.1.3	Beam (III)	28
3.2	York Steel Joists	29
3.2.1	Beam (IV)	36
3.2.2	Beam (V)	40
3.3	G.W.S. Joist	45
CHAPTER IV - ANALYSIS OF RESULTS		55
4.1	Theoretical Analysis	55
4.1.1	Beam Theory	55
4.1.2	Finite Element Analysis	58
4.1.3	Incomplete Interaction Theory	59
4.2	Steel Strains	64
4.3	Deflections	68
CHAPTER V - ULTIMATE STRENGTH DESIGN		71
5.1	Design Parameters	71
5.1.1	Effective Slab Width	71
5.1.2	Effective Slab Thickness	72
5.1.3	Strength of Connectors	74
5.2	Design Method	77
5.3	Load Factor	86
CHAPTER VI - SUMMARY AND CONCLUSIONS		91
6.1	General	91
6.2	Future Research	92
LIST OF REFERENCES		93

LIST OF TABLES

TABLE NUMBER		PAGE
1	SECTION PROPERTIES FOR JOISTS	14
2	DIMENSIONS OF BEAMS	14
3	PROPERTIES OF MATERIALS FOR BEAMS	15
4	PROPERTIES OF COMPOSITE SECTION	15
5	SECTION PROPERTIES FROM BEAM THEORY	57
6	WORKING LOAD CALCULATIONS (BEAM THEORY)	65
7	BOTTOM FIBRE STRAIN AT MID-SPAN UNDER WORKING LOAD	66
8	MID-SPAN DEFLECTION AT WORKING LOAD	69
9	ULTIMATE STRENGTH DESIGN	78
10	ULTIMATE MOMENT CALCULATION FOR TEST BEAMS USING DESIGN METHOD	84
11	ULTIMATE MOMENT CALCULATION FOR TEST BEAMS USING EXPERIMENTAL RESULTS	85
12	LOAD FACTOR FOR BEAMS	87
13	LOAD FACTOR FOR CONNECTORS	88

LIST OF FIGURES

FIGURE NUMBER		PAGE
1.1	OPEN-WEB COMPOSITE BEAM WITH RIBBED METAL DECKING	3
1.2	COST COMPARISON	9
2.1	TEST ARRANGEMENT	12
3.1	ANTHES JOIST (BEAM I)	21
3.2	FAILURE OF BEAM (I)	23
3.3	ANTHES JOIST (BEAMS II, III)	25
3.4	FAILURE OF BEAM (II)	27
3.5	FAILURE OF PUDDLE WELDS AT SUPPORT	30
3.6	FAILURE OF BEAM (III)	31
3.7	LOAD-DEFLECTION CURVES (BEAMS I, II, III)	32
3.8	LOAD VERSUS END SLIP (BEAMS I, II, III)	33
3.9	LOAD VERSUS STEEL AND CONCRETE STRAINS (ANTHES JOISTS)	34
3.10	STRAINS ACROSS THE X-SECTION (BEAMS I, II, III)	35
3.11	YORK STEEL JOIST (BEAM IV)	37
3.12	FAILURE OF BEAM (IV)	39
3.13	YORK STEEL JOIST (BEAM V)	41
3.14	LOAD-DEFLECTION (YORK STEEL JOISTS)	43
3.15	LOAD-VERSUS END SLIP (BEAMS IV, V)	44
3.16	LOAD VERSUS STEEL AND CONCRETE STRAINS (YORK STEEL JOISTS)	45
3.17	G.W.S. JOIST (BEAM VI)	48
3.18	DEFLECTION OF BEAM VI AT FAILURE	49

3.19	FAILURE OF BEAM VI	51
3.20	LOAD-DEFLECTION (BEAM VI)	52
3.21	LOAD VERSUS END SLIP (BEAM VI)	53
3.22	LOAD VERSUS STEEL AND CONCRETE STRAINS (BEAM VI)	54
4.1	TYPICAL CROSS-SECTIONAL PROPERTIES, FORCES AND STRAINS IN INCOMPLETE INTERACTION	60
4.2	LOAD VERSUS STEEL STRAIN (ALL BEAMS)	67
4.3	LOAD VERSUS DEFLECTION (ALL BEAMS)	70
5.1	LOAD VERSUS CONCRETE STRAINS (BEAM II)	73
5.2	LOAD FACTOR	90

NOTATIONS

A_c	effective concrete area
A_{sb}	area of bottom chord
A_{st}	area of top chord
a	depth of concrete stress block
b	slab width
C	compressive force in concrete slab at ultimate
C'	compressive force in top chord at ultimate
C_a	constant
C_b	constant
C_c	center of gravity of concrete slab
C_s	center of gravity of steel joist
C_{comp}	center of gravity of composite section
d	distance between C.Gs. of top and bottom chord
E_c	modulus of elasticity of concrete
E_s	modulus of elasticity of steel
e	lever arm of force C about C.G. of bottom chord
e'	lever arm of force C' about C.G. of bottom chord
F_c	force in concrete slab for incomplete interaction theory
F_{st}	force in top chord for incomplete interaction theory
F_{sb}	force in bottom chord for incomplete interaction theory
F_y	yield stress of steel

F_{act}	actual stress measured in steel
F_{ult}	ultimate stress of steel
f'_c	ultimate stress of concrete
G_b	distance from C.G. of bottom chord to its lowest point
G_t	distance from C.G. of top chord to its highest point
H	total height of test specimen
I_c	moment of inertia of concrete slab
I_{sb}	moment of inertia of bottom chord
I_{st}	moment of inertia of top chord
I_s	moment of inertia of steel joist
I_{comp}	moment of inertia of composite section
I_{full}	moment of inertia for a fully composite beam
I_{code}	moment of inertia according to code
I_{steel}	moment of inertia for a non-composite beam (I_s)
K	connection shear modulus
L	span of test specimen
M	bending moment
M_c	bending moment in concrete slab
M_{full}	moment capacity for a fully composite beam
M_{code}	moment capacity according to code
M_{steel}	moment capacity for a non-composite beam
M_{ult}	ultimate moment
ΔM	increase in moment capacity
M_x	bending moment at distance x
N	number of connectors provided
N_u	number of connectors needed to achieve full ultimate flexural capacity

n	modular ratio
P_w	working load
P_y	yield load
P_{cr}	critical buckling load
Q	connector load
Q_u	ultimate capacity of connector
q	Q/s
s	average distance between connectors
T	tension in bottom chord at ultimate
T'	tension in top chord at ultimate
T'_y	tension in top chord at yield
t	total thickness of slab
t_r	thickness of ribbed part of slab
t_s	thickness of solid part of slab
U	distance from load point to support
v	$\sqrt{C_a \cdot K/S}$
W	total load on beam
x	distance
Y_c	distance from C.G. of slab to C.G. of composite section
Y_{sb}	distance from C.G. of bottom chord to C.G. of composite section
Y_{st}	distance from C.G. of top chord to C.G. of composite section
Y_s	distance from C.G. of steel joist to C.G. of composite section
Y	distance from C.G. of bottom chord to C.G. of steel joist

γ_{full}	γ_{sb} for a fully composite beam
γ_{code}	γ_{sb} for a section reduced according to code
γ_{steel}	γ_{sb} for a non-composite beam (γ_s)
α	$\frac{nA_{sb} \cdot d^2}{I_c}$
β	$\frac{A_{sb}}{A_{st}}$
γ	slip
ϵ	strain
ϵ_c	concrete strain
ϵ_{sb}	bottom chord steel strain
ϵ_{st}	top chord steel strain
ϵ_w	steel strain at working load
ϵ_y	steel strain at yield
ϕ	curvature
η	$-\frac{dy}{dx}$

CHAPTER I

INTRODUCTION

1.1 COMPOSITE BEAMS

Structural floors composed of a concrete slab and supporting steel beams are extensively used in construction.

When these two components are just resting, one on top of the other, their combined carrying capacity is the sum of the carrying capacity of each separately.

By interconnecting them in a way which causes horizontal shear transfer from one element to the other, the carrying capacity of the system increases considerably.

The most common way of providing composite action for this type of construction is by welding shear connectors to the top of the steel beam and embedding them in the concrete slab. These composite steel and concrete beams were generally used in bridge construction until recently when they started to be used in buildings.

With their introduction in buildings other considerations than low cost and structural soundness had to be studied.

The major new factors to be incorporated in the design, especially in the case of office buildings, were the accommodation of services within the floor and the provision of a flexible interior design.

This led to the replacement of the usual rolled steel joist by open web steel joists or trusses. Ribbed metal dec-

king is used as in situ formwork for the concrete slab and reduces the time and cost of construction. The decking acts as walking surface during construction and eliminates the shuttering.

The resulting floor, a composite beam system composed of a concrete slab, with a solid part and a ribbed part encased in metal decking, and an open web steel joist is shown in Fig. 1.1.

The connectors are welded to the top chord of the joist through the decking and protrude a certain distance into the solid part of the slab.

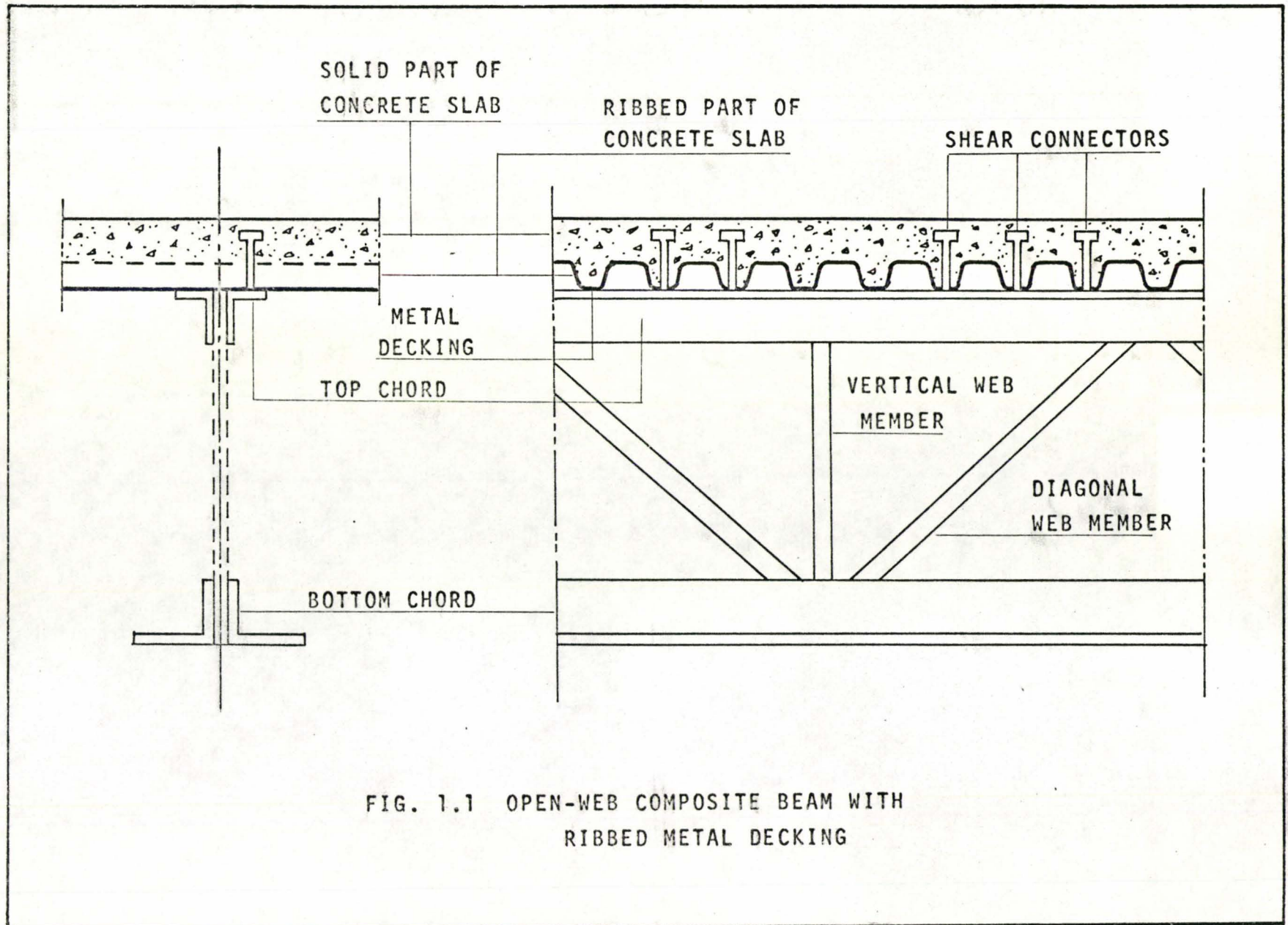
1.2 PREVIOUS RESEARCH

A considerable amount of experimental and theoretical research has been conducted on conventional composite construction.

Siess, Viest and Newmark⁽¹⁾ conducted a large number of push-out and beam tests and concluded that the stiffer the connection, the greater the shear carried and the higher the degree of composite action attained.

They also developed a differential equation for incomplete interaction for a general case of a beam consisting of two interacting elements.

They suggested that the modulus of the shear connectors, the only term in the derived equations which is not known from the dimensions of the beam and the properties of the material may be determined experimentally from push-out tests.



Slutter and Driscoll⁽²⁾ reported tests on composite steel and concrete beams with different types and arrangement of shear connectors.

They proposed a method of determining the ultimate bending capacity of beams with a weak shear connection and obtained good correlation with the experimental results. They stressed the relationship between the ultimate strength of the shear connectors and the ultimate strength of the beam.

They came to the conclusion that if enough shear connectors were provided, the theoretical ultimate moment could be attained even with the presence of appreciable slip; and also that the ultimate flexural capacity of a beam could be determined even if the number of shear connectors provided was less than the number required to develop the maximum theoretical ultimate bending moment.

While much more research has been done on this conventional type of composite beam, it was only recently that composite open-web steel joists were investigated. Most of that work was done by Galambos^(3,4) who described tests on cantilevers and simply supported composite trusses.

His first report mainly evaluated the capacity of the shear connectors determined from tests on cantilevers and simply supported beams consisting of solid concrete slabs and open-web steel joists. The incomplete interaction equation developed by Newmark was extended for this type of composite system.

A second report⁽⁴⁾ described tests on five open-web composite steel joists with 3/8 in. stud shear connectors; it was demonstrated that the ultimate test load was well predicted by the load at which the bottom chord of the joist reached its theoretical yield stress. A design procedure based on elastic theory was described. In this design method; the critical element, the bottom chord, was designed for a tensile stress of $0.6 F_y$ and a factor of safety of 2.5 was suggested for the design of connectors.

The introduction of ribbed metal decking in the composite system was investigated by Robinson. His first beam test spanned 21 feet and had 3/4 in. studs. He concluded in the report on the test⁽⁵⁾ that the system was effective, having obtained a stiffness for the composite system in the elastic range 3.75 times that for the steel beam alone.

He recommended the use of only the solid part of the slab as resisting compressive stresses in designing the composite system.

He also stated that the loss of interaction results from two components of slip; slip at the intersection of the deck and the steel beam similar to the one arising in conventional composite beams and another major component resulting from rotation of the ribs.

Robinson proposed a method of establishing design criteria for composite beams incorporating cellular steel decking in 1964⁽⁶⁾, by using load slip results together with the New-

mark theory. The method was supported by observations from a variety of tests and he concluded as did Galambos that the most accurate evaluation of connector performance can be obtained from tests on beams which are intentionally constructed with few connectors to ensure connection failure before yielding of the beam. To investigate the influence of the rib geometry and other factors on the load deflection characteristics, he performed tests on 15 beams and 39 push-out specimens⁽⁷⁾.

His conclusions were that the overall behaviour of the beams was not affected by different stud diameter and spacing, and that the governing criterion was the geometry of the ribs. He found that a rib height-to-width ratio equal to one produced rib-cracking closely following local yielding of the beam. With a larger rib height-to-width ratio the cracking of the ribs occurred in the elastic range and with a smaller one, a load in excess of first yield could be achieved.

The computation of the ultimate moment for a composite beam with ribbed metal decking and its verification by test results was described in references (8) and (9).

1.3 ADVANTAGES AND ECONOMICS OF THE SYSTEM

The general advantage of composite construction over ordinary non-composite construction is an increase in stiffness and therefore less deflection for the same load and span.

The structural advantage of using an open-web joist instead of a rolled section is to make the system lighter, by

increasing the moment arm between the tension and compression zones, thus achieving larger spans.

Other architectural, economical and practical advantages also result from this substitution. The openings in the joist are adequate for accommodating mechanical and electrical services particularly prevalent in office buildings. They also allow for easy access to these services, thus reducing maintenance costs. Means for heat and moisture insulation, fireproofing and noise damping materials are easily accommodated. Lighting fixtures and other ceiling attachments can be installed without any difficulty. The introduction of ribbed metal decking results in definite savings in shuttering and forms, reducing construction time and cost.

The number of ribs is usually large enough to receive the number of connectors necessary for full composite action.

The system as a whole has dynamic properties far superior to those of a non-composite open-web joist system and although a dynamic investigation is still underway one can safely state that the natural frequency is greatly increased.

As for the economy achieved by savings in material, the size of the top chord in this system is smaller than the bottom chord, whereas in non-composite joists the contrary is the case. Although this economy is somewhat offset by the additional cost of the shear connectors, an economic study⁽¹⁰⁾ shows that the system becomes more economical than a non-composite joist system for spans of 37 ft. and greater. For

example at a span of 60 ft. the cost per square foot of installed floor is \$2.12 for the composite floor against \$2.52 for the non-composite floor (Fig. 1.2).

1.4 OBJECT OF RESEARCH

The aim of this research is to determine a sound design method for open-web composite joists with metal decking.

The different parameters affecting the design which have to be studied are:

- the actual connector strength in the beam and whether it is of the same value as the one obtained from push-out tests
- the effective width of the slab acting in compression with the composite section
- the effective thickness of the concrete
- the flexibility of the shear connectors
- the transfer of compressive stresses from joist to slab at different stages of loading and the failure mechanism of the system
- the effects of the reduction of the number of shear connectors from that needed to achieve full ultimate flexural capacity
- the behaviour of the beams when using different shear connectors with different flexibility and strength.

After studying the effect of these factors on the behaviour of the system and establishing design criteria; exact analytical methods have to be evaluated as to their

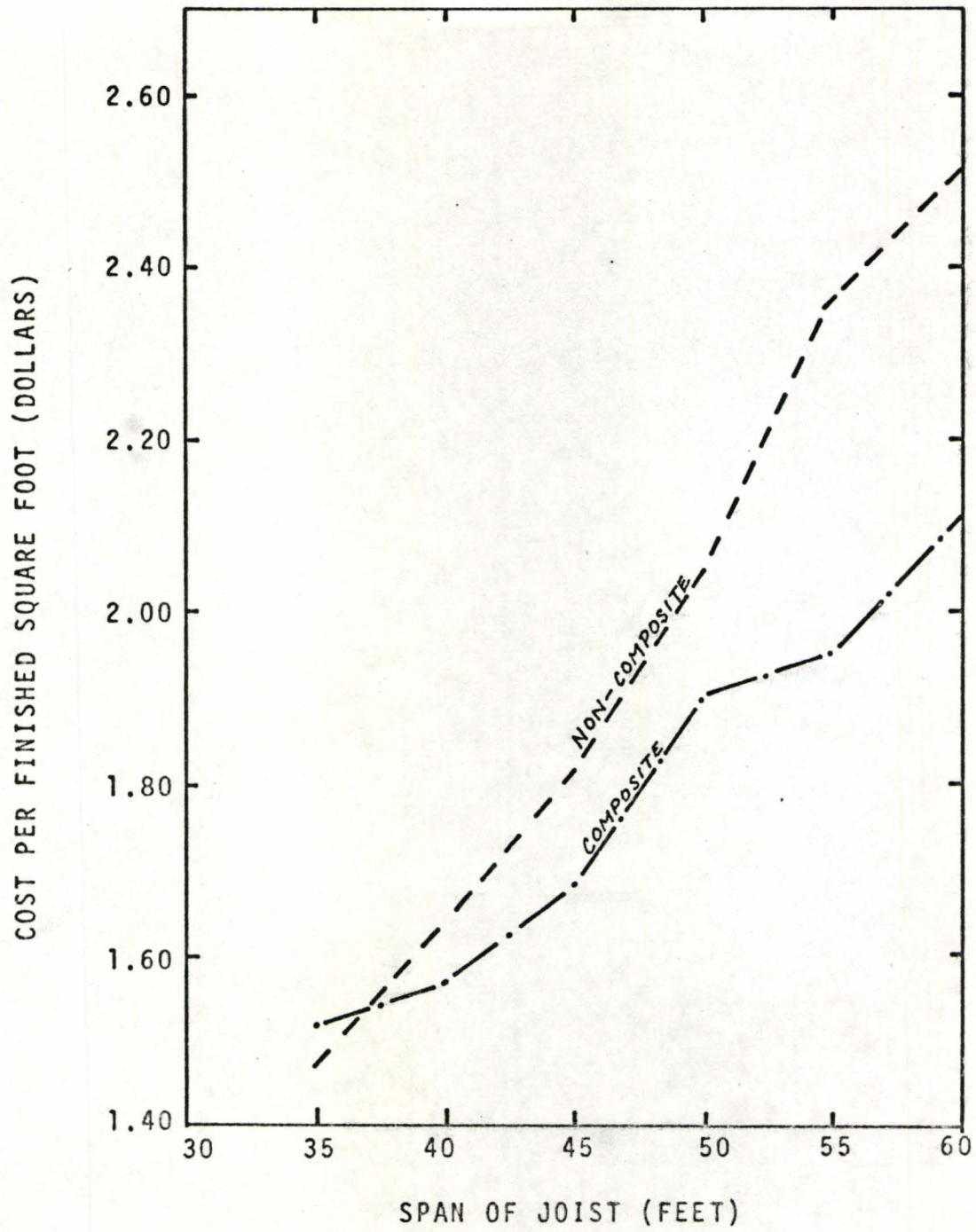


FIG. 1.2 COST COMPARISON

prediction of the behaviour of the beams. These methods necessitating lengthy derivations and the use of an electronic computer cannot always be followed for ordinary design purposes and a simpler design procedure has to be derived.

CHAPTER II

DESCRIPTION OF TESTS

2.1 TEST SPECIMENS

A total of six beam tests were performed. The 50 ft. span beams were simply supported at the ends and they were loaded through the top of the slab by two equally spaced concentrated loads $W/2$, giving a central moment span and two shear spans at the ends (Fig. 2.1). Three types of joist were used for the beams; namely for Beams I, II and III Anthes cold rolled joists, for Beams IV and V York Steel hot rolled joists and for Beam VI a Great West Steel joist.

The data pertinent to the six test joists, their cross-sectional properties and materials are given in Tables 1, 2, 3 and 4.

Each type of joist had its own distinctive chord configuration. For the Anthes joist the top and bottom chord were V10 and V14 of Anthes 3 in. V sections and the web members were Anthes o.s. tubes.

The York Steel joists were composed entirely of standard size angles.

The G.W.S. joist had hat shaped chords while the web members were tubes.

In all test joists the bottom chords had larger area

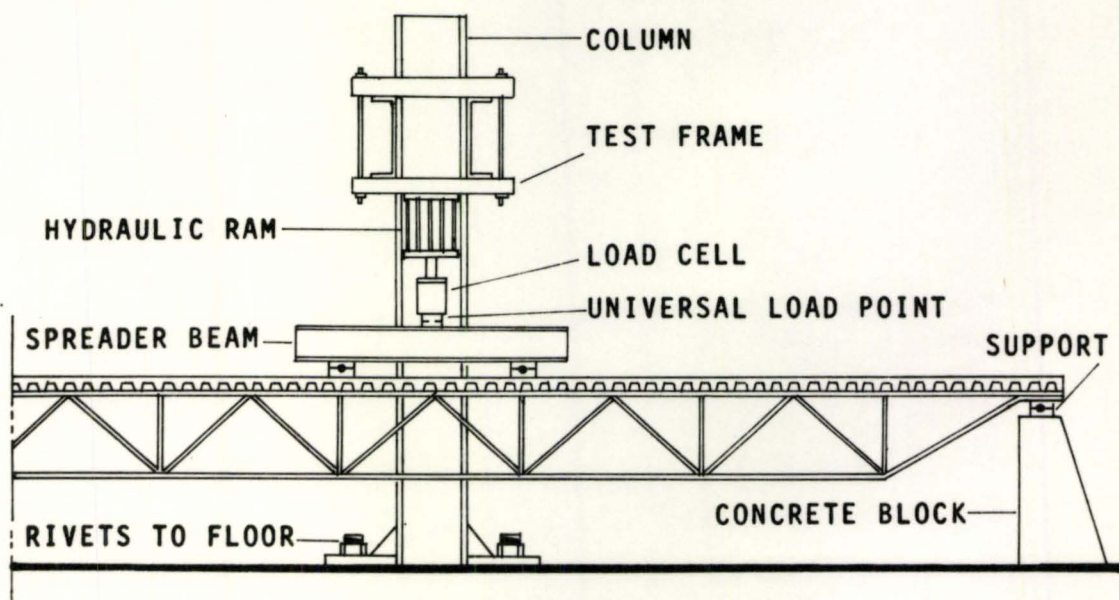
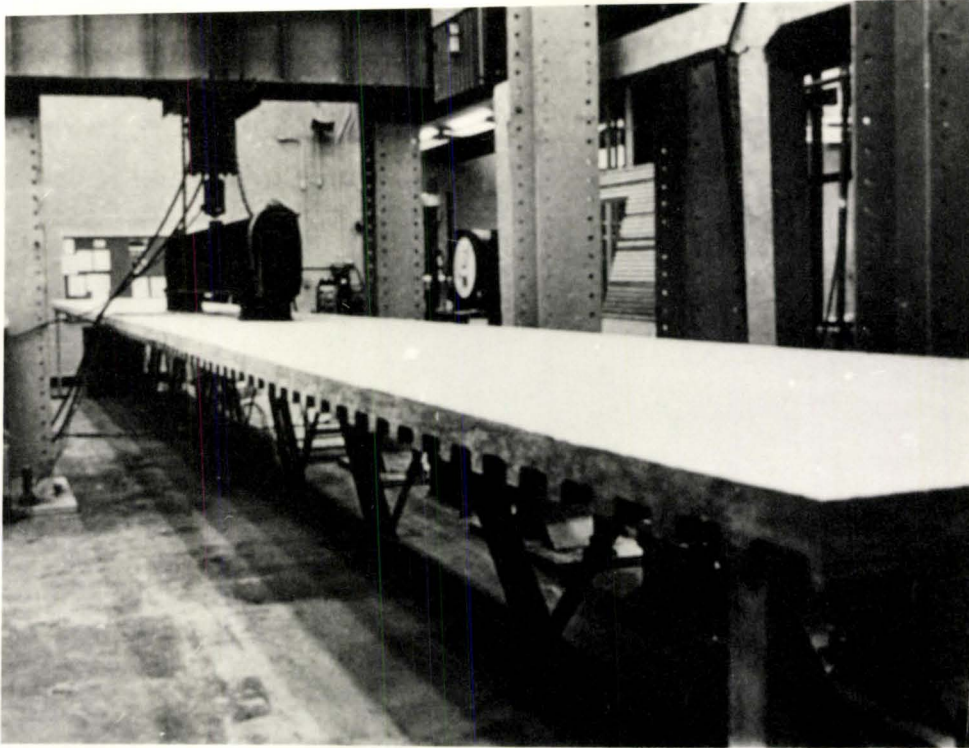


FIG. 2.1 TEST ARRANGEMENT

than the top chords except for Beam V. The size of the web members was intentionally increased to avoid failure due to web buckling, and they were so designed as to achieve failure by tension chord yielding in the central moment span. This is shown in the calculations. The steel had a modulus of elasticity of 29,000 k.s.i. and the required minimum yield stress varied from type to type.

The concrete slab was poured in 1.5 in. cellular metal decking with a 6 in. rib spacing module. The slab width was 5 ft. and the solid part above the ribs was 2.5 in. thick.

The concrete used was ready-mixed required to give 3 k.s.i. at 14 days and to have a 3 in. slump. It was reinforced with a 10 x 10 gauge welded wire mesh with 6 in. x 6 in. spacing.

The concrete was wet cured for 7 days.

Six cylinders, cured alongside the slab, were tested on the same day of the beam test.

The connectors for Beams I, II and IV were Nelson studs which were welded through the metal decking to the flanges of the top chord.

The total stud height was 3 in. and the diameter was 1/2 in. for Beams I and II and 3/4 in. for Beam IV.

The studs were as evenly spaced as possible and alternated on both flanges of the top chord.

For Beams III, V and VI the decking was puddle welded to the joist, at each rib location for Beam III, at every al-

NOTE: BEAM STANDS FOR THE JOIST + SLAB

Beam No.	A_{ST} (in ²)	A_{SB} (in ²)	A_C (in ²)	I_{ST} (in ⁴)	I_{SB} (in ⁴)	I_C (in ⁴)	G_T (in)	G_B (in)
I	1.84	2.85	150	1.89	2.86	78.12	1.03	0.96
II	1.84	2.85	150	1.89	2.86	78.12	1.03	0.96
III	1.84	2.85	150	1.89	2.86	78.12	1.03	0.96
IV	2.62	2.88	150	2.30	1.60	78.12	0.91	0.61
V	3.56	2.88	150	4.40	1.60	78.12	1.14	0.61
VI	1.76	1.99	150	0.35	0.39	78.12	0.51	0.54

TABLE 1 SECTION PROPERTIES FOR JOISTS

Beam No.	Span L(ft)	Load Pt. u(ft)	Height of Joist H(in)	Type of Joist	Width of Slab b(ft)	Thickness of Slab t(in)
I	51.00	21.50	32.00	Anthes	5.00	4.00
II	51.00	21.50	32.00	"	5.00	4.00
III	51.00	21.50	32.00	"	5.00	4.00
IV	50.00	20.00	32.00	York Steel	5.00	4.00
V	50.00	20.00	32.00	"	5.00	4.00
VI	50.00	21.00	32.00	G.W.S.	5.00	4.00

TABLE 2 DIMENSIONS OF BEAMS

Beam No.	F_{s_y} k.s.i.	$F_{s_{ULT}}$ k.s.i.	F'_c k.s.i.	E_s k.s.i.	E_c k.s.i.	n
I	60.7	66.0	3.30	29×10^3	3.3×10^3	8.80
II	60.7	66.0	4.20	29×10^3	3.72×10^3	7.80
III	60.7	66.0	3.70	29×10^3	3.5×10^3	8.30
IV	59.2	-	4.65	29×10^3	3.92×10^3	7.40
V	59.2	-	3.55	29×10^3	3.42×10^3	8.50
VI	60.0	-	4.80	29×10^3	3.95×10^3	7.35

TABLE 3 PROPERTIES OF MATERIALS FOR BEAMS

Beam No.	A_{COMP} in ²	I_{COMP} in ⁴	Y_C in	Y_{ST} in	Y_{SB} in	Y_S in
I	21.69	2792.00	4.75	0.97	29.04	17.23
II	24.00	2831.00	4.30	0.52	29.49	17.68
III	22.79	2805.00	4.66	0.88	29.13	17.32
IV	25.70	2953.00	4.20	0.54	29.94	15.41
V	24.04	2849.00	4.67	0.47	29.78	12.72
VI	24.15	2174.00	3.05	0.21	31.17	16.61

TABLE 4 PROPERTIES OF COMPOSITE SECTION

ternate rib for Beam V and twice at each rib for Beam VI.

All connector and puddle welds were done in the laboratory after the joist was in the test position.

The decking was shored at several points along its length during pouring of concrete and the shoring was removed immediately after the pour except for the four props at the corners of the slab.

2.2 TESTING PROCEDURE

All beams were prepared, instrumented and had their slabs poured at the exact locations where they were tested.

The end conditions were simple supports. The supports were 2 in. diameter steel rollers resting on steel plates fixed on top of specially cast abutment type concrete blocks.

The load was applied by means of one 100,000 lb. hydraulic ram through a load cell to a spreader beam giving a two point symmetric loading. The load cell was calibrated immediately before and after each test.

The beams were instrumented to measure the load applied, the deflections at mid-span and under both load points, the slip between the concrete slab and the joist at the ends and at some intermediate points, the strains in the concrete slab at mid-span and at the load points on several locations along its transverse axis, and the strains at several points on the top and bottom chords and on some web members of the joists.

The load was read, by means of a digital voltmeter connected to the load cell, with an accuracy up to 20 lbs.

Deflections were measured by means of one-thousandth of an inch dial gauges.

All deflection and strain gauges were connected prior to the pour to record the effect of the dead loads.

Slips between the top chord of the joist and the concrete slab were measured with one-ten-thousandth of an inch dial gauges.

The gauges were attached to a bracket welded to the top chord with the plunger bearing either directly against the concrete at the locations on the ends of the beam or against an angle glued to the metal decking at other locations.

Concrete strains were measured using paper-backed electric resistance filament strain gauges 6 in. long, and were read by means of a manual strain indicator.

The steel strains were measured by 1/4 in. electric resistance foil strain gauges and recorded by a datran automatic digital recorder.

The locations of the electrical strain gauges on concrete and steel are described in Chapter III. Load was generally applied by increments of one kip up to yield and then deflection increments usually of half an inch were used.

After the application of each increment of load or deflection, readings of strains, deflections and slips were recorded. In the non-linear region the reading was done only

after the load stabilized. In addition to the above-mentioned recordings, the test specimens were carefully inspected during and after each load or deflection increment for any cracks in the concrete or any signs of failure.

CHAPTER III

TEST RESULTS

3.1 ANTHES JOISTS

Specimens I, II and III were anthes joists. The three joists were especially fabricated for the experimental program.

The top and bottom chords, made from anthes 3 in. V-sections were types V10 and V14 respectively and the web members were open-seam tubes.

All members were cold roll formed from coils of hot rolled steel strip.

The joists were manufactured with a built-in camber of 1 in.

Complete panel lengths of the bottom chord were tested in tension and the yield and ultimate stresses of the steel were found to be 60.7 and 66.0 k.s.i. respectively.

Fig. 3.1 shows an elevation of an Anthe's joist and cross-sections with gauge locations.

3.1.1 BEAM (I)

Beam (I) was provided with the required number of connectors to achieve full ultimate flexural capacity (29 studs in each shear span).

An additional 2 studs were welded on each side of the centre line in the constant moment region to prevent the slab

from lifting from the top chord under loading, on all beams with stud connectors. The connectors were 1/2 in. diameter nelson studs 3 in. long and welded at rib locations in a staggered pattern. The steel joist was instrumented with 26 strain gauges. The concrete slab had 6 filament gauges. Deflections were recorded at 3 locations under the load points and at mid-span and 3 slip gauges were placed at the two ends and on the second vertical from the east support. Connector pattern and gauge locations are shown in Fig. 3.1. The only readings due to dead load were the deflection, which was 1 in. for all Anthes joists and was taken care of by the built-in camber, and the steel strains whose maximum values in the top chord were of the order of 500×10^{-6} in./in. which corresponded to stresses below 25% of the yield.

The beam was first loaded in load increments of 2.0 kips. The load readings were recorded at the time of reading the gauges and immediately prior to the next application of load. The load remained steady after each increase up to 14.0 kips when it started dropping by small amounts of 0.2 to 0.4 kips after each loading step.

Deflections increased elastically under the two load points and at mid-span. The load-deflection relationship started deviating from a straight line at a load of 24.0 kips. The deflection increments became noticeably large at a load of 36.0 kips and the testing then proceeded by adding 0.5 in. increments of deflection instead of load. When the test spe-

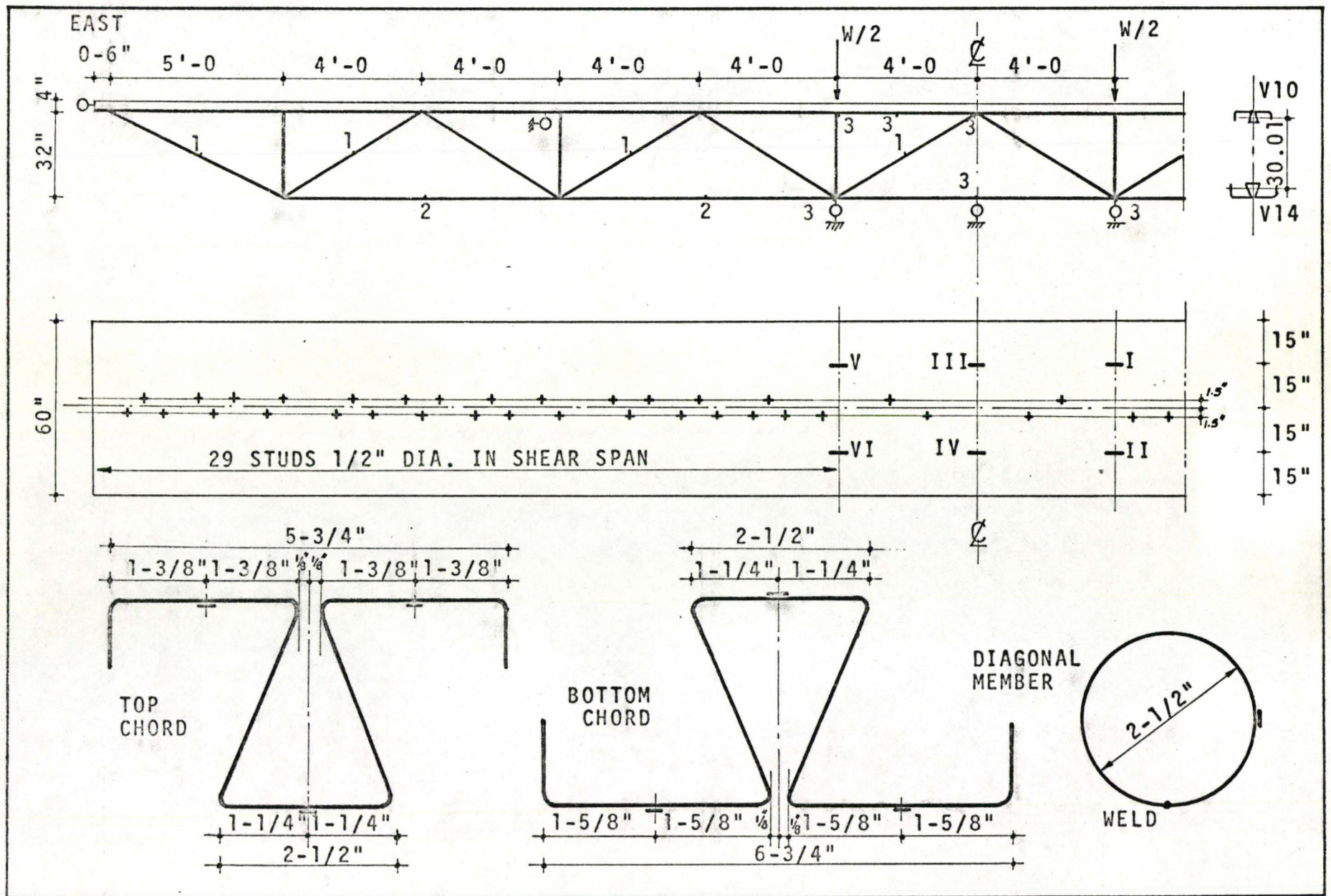


FIG. 3.1 ANTHES JOIST (BEAM I)

cimen failed it had already deflected 9 in. at mid-span (Fig. 3.7).

The slip at the two ends increased at a very slow rate up to 26.0 kips when the increments got larger. The slip at the second vertical was almost non-existent up to a load of 20.0 kips when it started increasing but still at a lower rate than that at the ends.

The steel strain readings indicated that yielding started in the bottom chord under the load points at a load of 30 kips. The compressive strain in the flange of the top chord remained almost constant and equal to its value under dead load up to a load of 40 kips when it increased rapidly to reach a maximum value at failure of one and a half times its value under dead load.

The diagonal members in the constant moment region remained in compression from the start up to a load of 35 kips when they went into tension.

The truss continued to take increasing load after the onset of yield in the bottom chord until the specimen failed by fracture of the bottom chord at the joint under the west load point at a load of 41.2 kips. The steel had reached its ultimate stress. This was confirmed by the ultimate moment calculations.

Concrete strains were similar at all locations during loading and only very near ultimate did strains at mid-span exceed the ones measured under the load points. The concrete

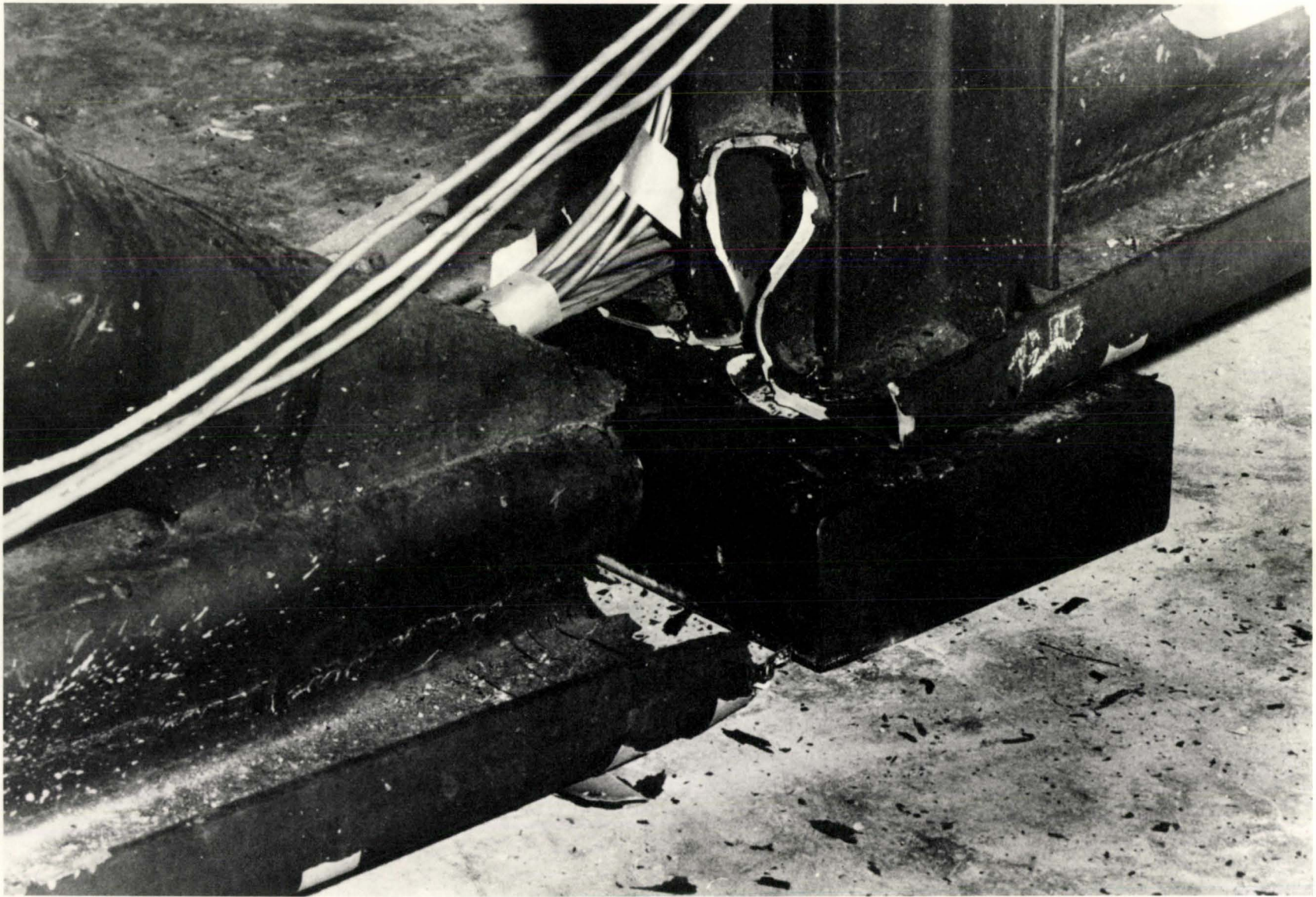


FIG. 3.2 FAILURE OF BEAM (I)

showed a few hair cracks at the upper corners of the ribs in the region of maximum moment immediately prior to failure of the specimen.

There were no signs of connectors punching through the metal deck and no other signs of damage were seen up to failure.

Beam I reached its theoretical ultimate moment and behaved as predicted. Its failure was by pure tension in the bottom chord as is clear from Fig. 3.2.

3.1.2 BEAM II

Beam II was only provided with half the number of connectors required to achieve full ultimate flexural capacity (15 studs, 1/2 in. diameter in each shear span).

The steel joist was instrumented with 19 strain gauges. The concrete slab had 8 strain gauges placed in such a way as to evaluate the effective width. Deflection gauges were placed under the load points and at mid-span and slip was only measured at the two ends.

Connector pattern and location of gauges are shown in Fig. 3.3.

The beam was loaded with 1.0 kip load increments. The load remained fairly steady between consecutive applications up to 20.0 kips and then dropped small amounts of about 0.3 kips.

The load deflection relationship remained linear up to a load of 17.0 kips and then deviated rather abruptly.

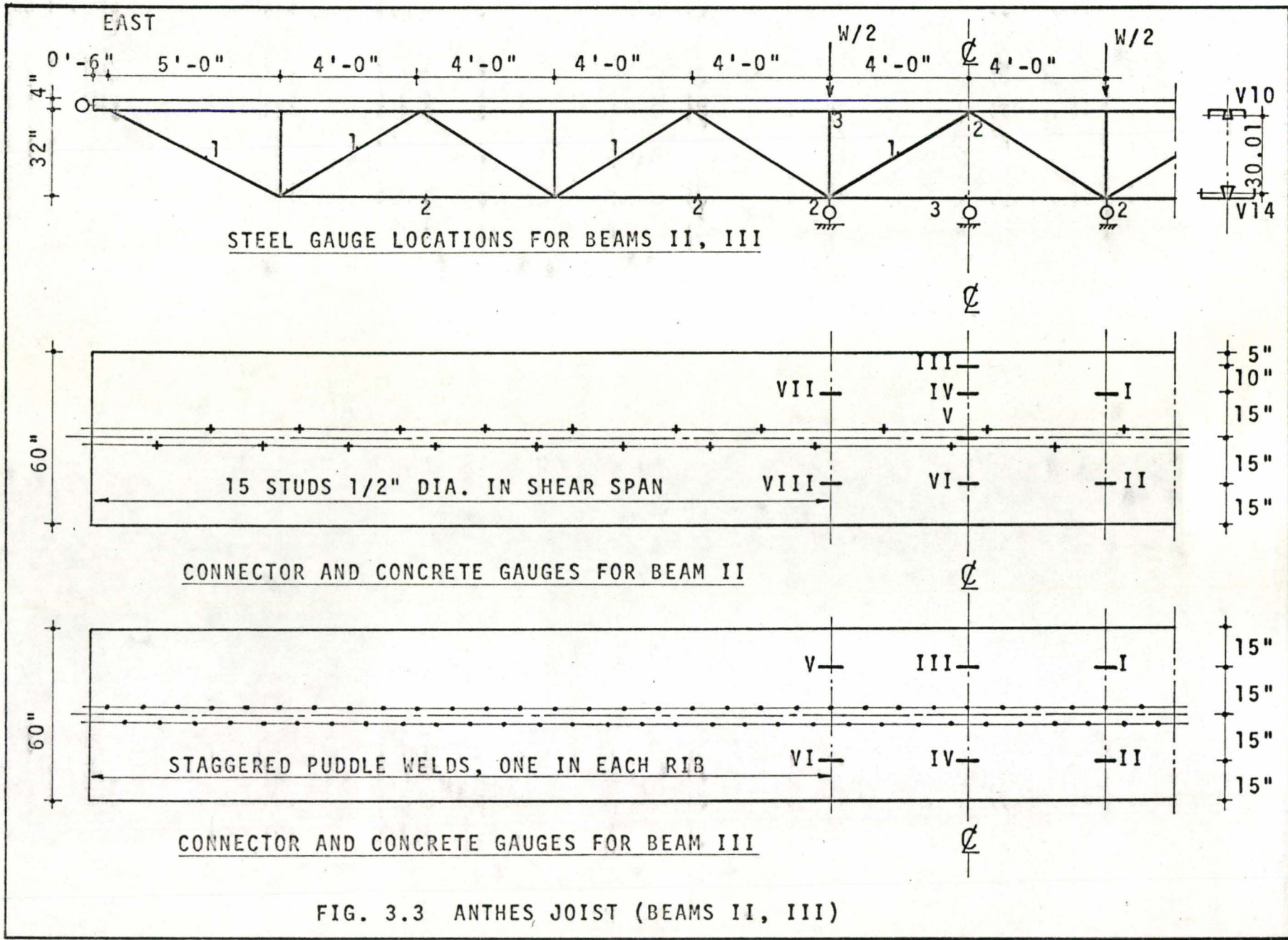


FIG. 3.3 ANTHES JOIST (BEAMS II, III)

At failure the total deflection at mid-span due to the test load was 6 inches (Fig. 3.7). The slip readings at the east and west ends of the beam increased at a similar rate up to a load of 24.0 kips when the west slip started increasing at a much faster rate so that at 29.0 kips it was already twice as much as the east slip. The same observation was made on deflection and strain readings but to a lesser extent.

Steel strains in the bottom chord followed a perfect straight line relationship with load up to 18 kips and the yielding of the bottom chord occurred at a load of 27.0 kips.

The compressive strains in the joist's top chord decreased slightly to reach a minimum at a load of 10.0 kips and then increased again and were equal to their value under dead load at a load of 20.0 kips.

With subsequent increase in load the compressive strains increased to values much higher than the ones reached in Beam I, so that at failure their value was three times that reached under dead load. The middle diagonal remained in compression all through the test at an almost stable value. Concrete strains were higher at load points than at mid-span. The readings of the four gauges at mid-span were similar all throughout the test. Strain readings under the west load point became noticeably larger than the ones under the east load point at a load of 18.0 kips.

The specimen failed by buckling of the top chord in



FIG. 3.4 FAILURE OF BEAM II

the panel west of the west load point at a test load of 34.6 kips (Fig. 3.4).

3.1.3 BEAM III

The shear connection in Beam III was achieved by welding the metal deck to the top chord of the joist. One puddle weld was made at each rib in a staggered pattern.

The steel joist was instrumented with 19 strain gauges placed at the same locations as for Beam II. The concrete slab had 6 strain gauges, 2 under each load point and 2 at mid-span. Deflections were also recorded at these locations and slips at the two ends of the beam (Fig. 3.3).

The loading was applied by increments of 1 kip from the start up to a load of 10.0 kips and then changed to increments of 2.0 kips.

The load was dropping from 0.2 to 0.3 kips between loading after a load of 18.0 kips.

The load-deflection relation followed a straight line up to a load of 14.0 kips and then deviated slightly up to failure without ever reaching a plateau phase.

The deflection at failure due to the test load was 2.4 inches.

Slip, increasing at a lesser rate than for Beams I and II, was of equal value at the two ends and only increased suddenly at failure on the east end due to the failure of the puddle welds on that side.

Steel strains in the bottom chord followed a straight line relationship from the start of loading to the point of failure.

The steel strain at failure was 1900×10^{-6} in./in. in the flange of the bottom chord, equivalent to a stress of 55 k.s.i., which is below the yield stress of the steel.

The compressive strains in the joist top chord remained equal to their value under dead load up to failure of the welds and then tripled in value.

Concrete strains were equal at all locations and well below those of Beams I and II.

At a load of 24.0 kips sounds were heard indicating failure of welds. This continued during the next 3 loadings and just before failure of the beam a series of puddle welds had failed near the east support and the slab started lifting from the joist (Fig. 3.5).

During the last loading step all the welds on the east shear span failed and at the same time the top chord of the joist buckled over a whole panel length on the beam's east side (Fig. 3.6). The maximum load that had been reached was 29.6 kips.

3.2 YORK STEEL JOISTS

York steel joists were used for Beams IV and V. The joist members were formed of standard angles or plates.

The steel for the joists was hot rolled and tensile



FIG. 3.5 FAILURE OF PUDDLE WELDS AT SUPPORT



FIG. 3.6 FAILURE OF BEAM III

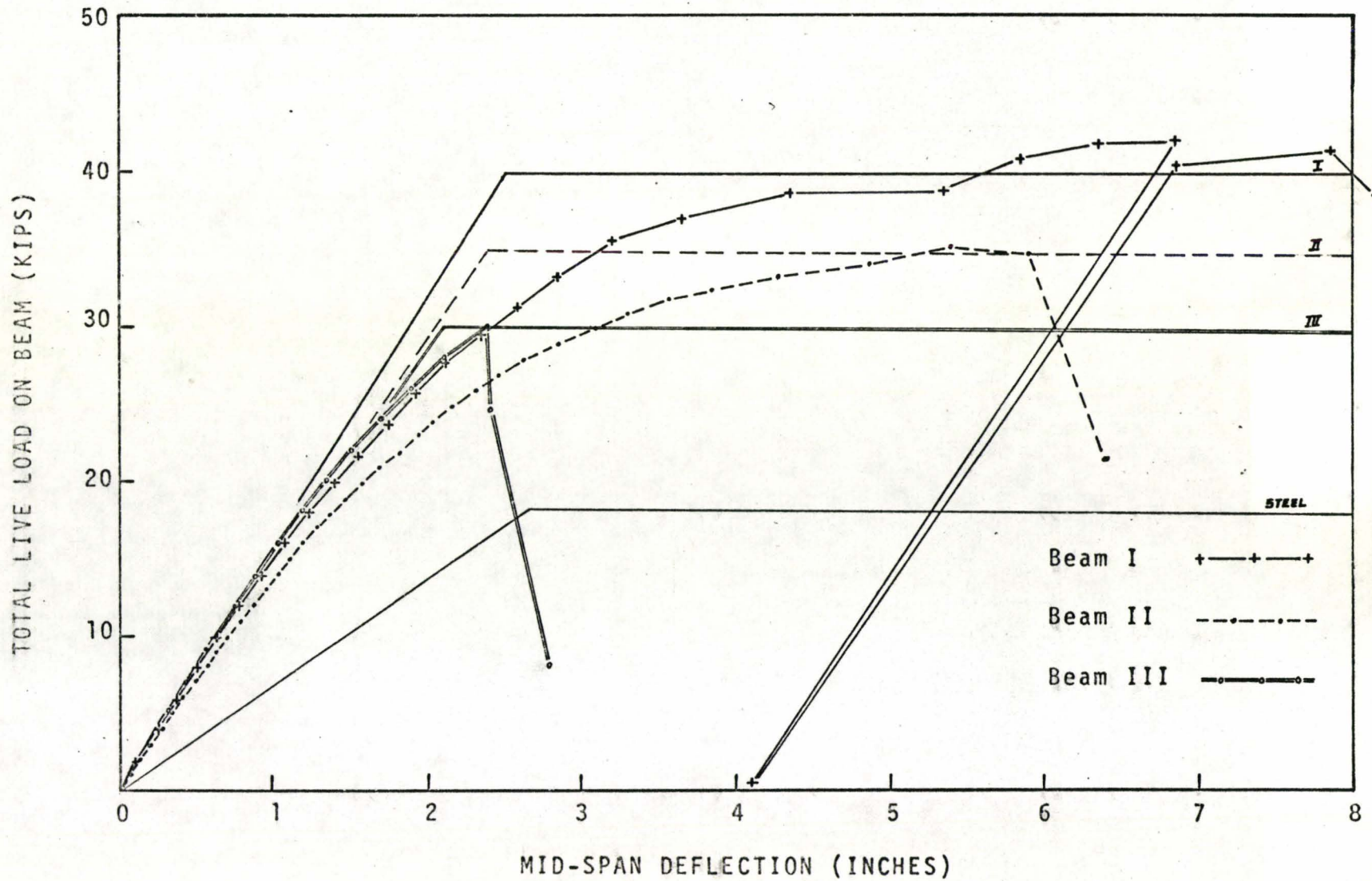


FIG. 3.7 LOAD DEFLECTION CURVES (BEAM I, II, III)

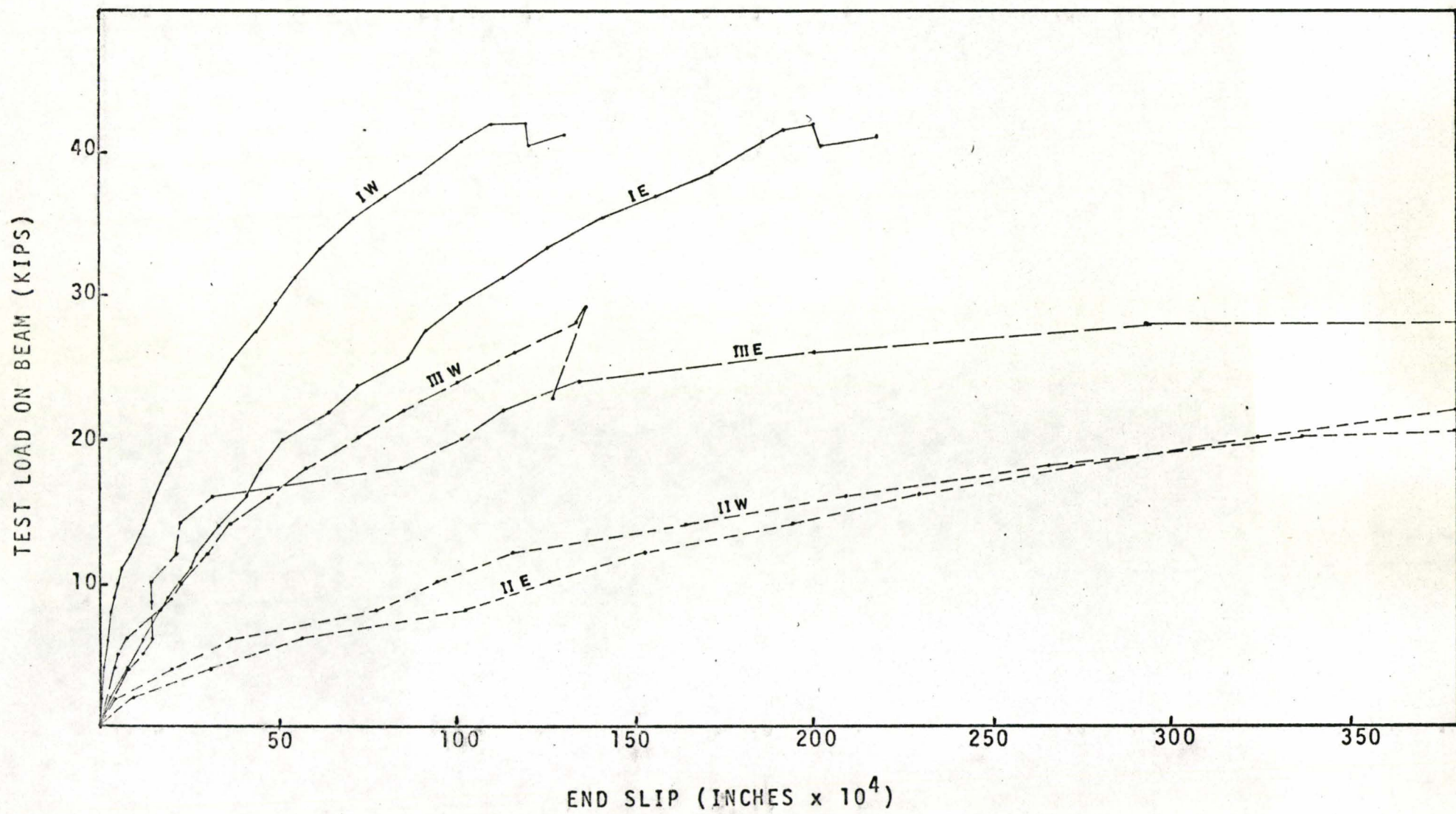


FIG. 3.8 LOAD VERSUS END SLIP (BEAMS I, II, III)

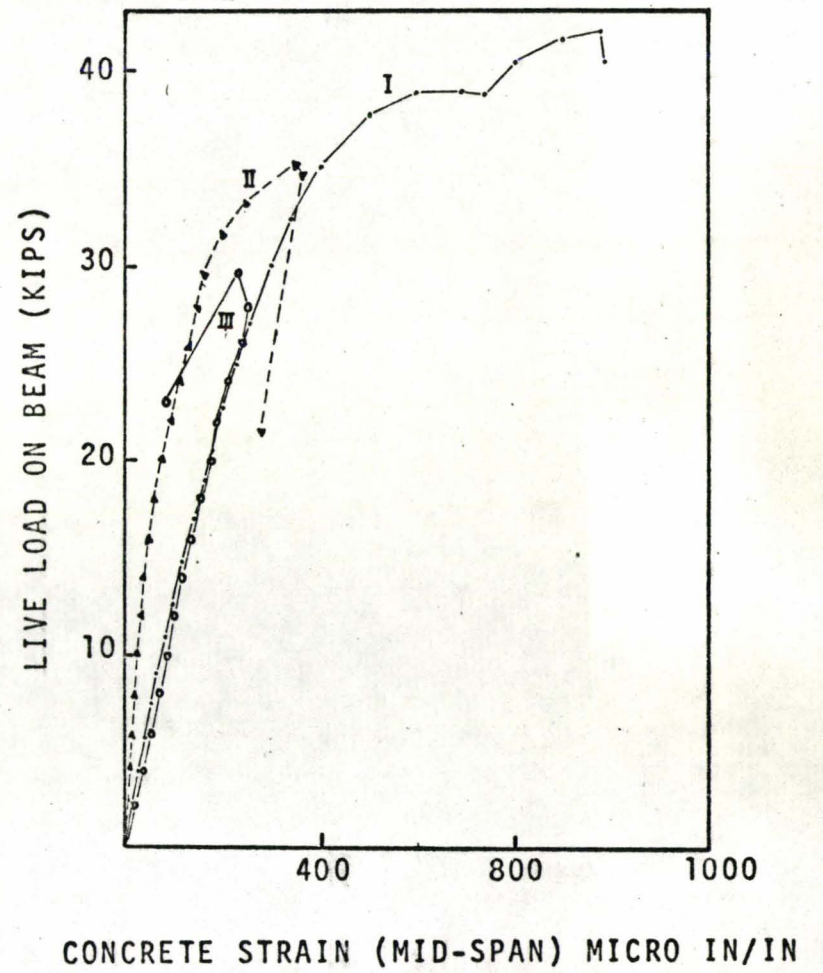
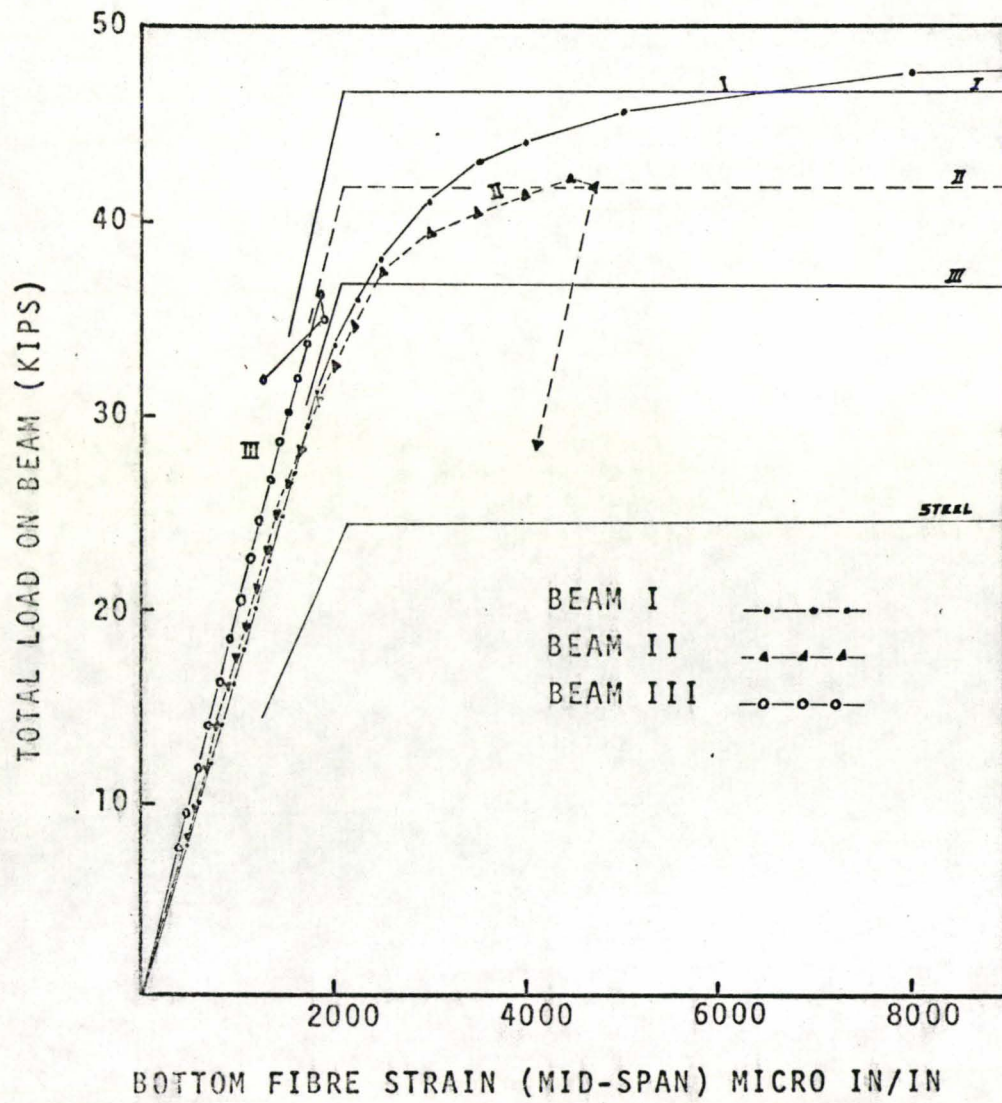


FIG. 3.9 LOAD VERSUS STEEL AND CONCRETE STRAINS (ANTHE'S JOISTS)

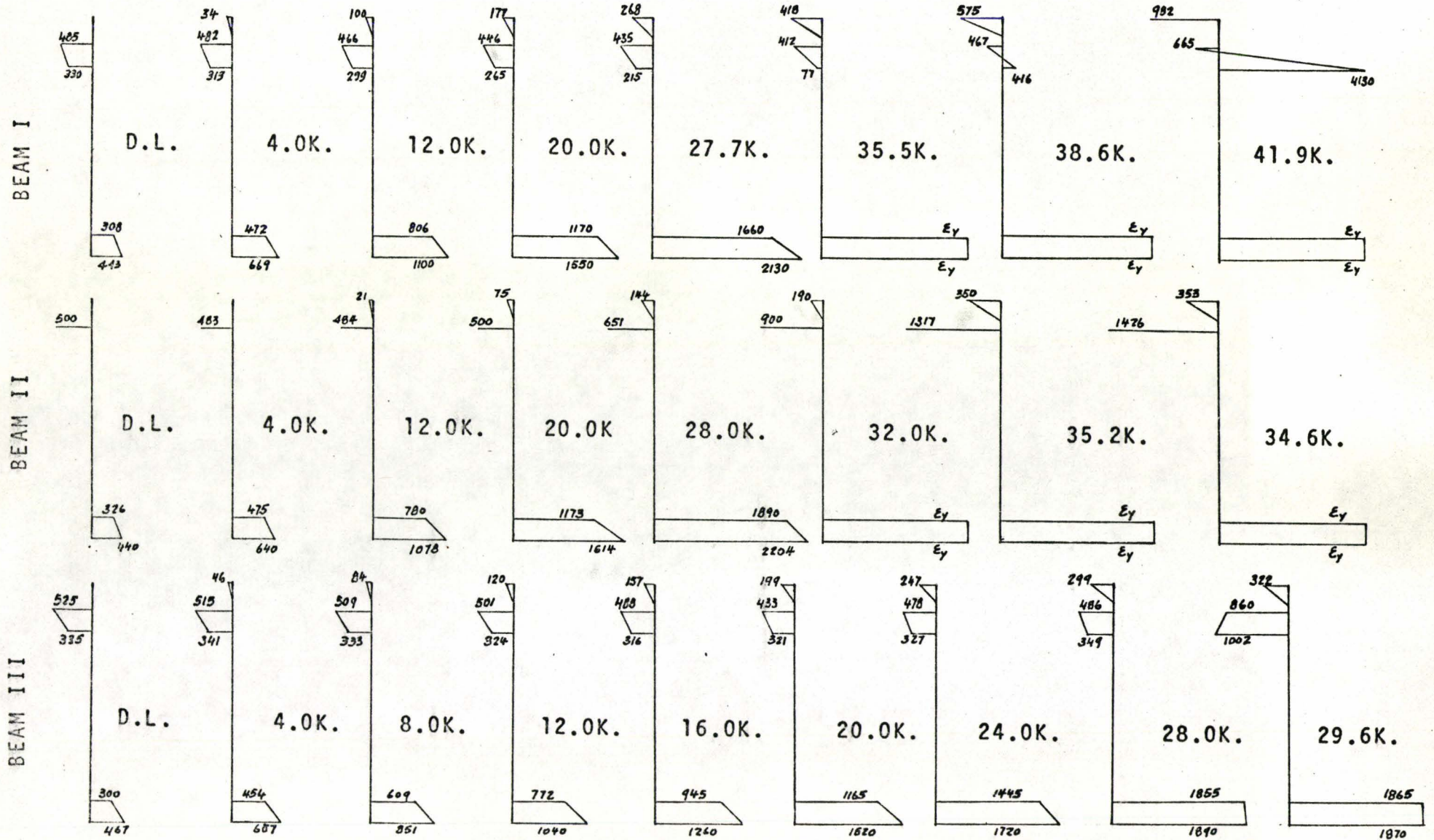


FIG. 3.10 STRAINS ACROSS THE X-SEC. (BEAMS I, II, III) AT MID-SPAN

tests on steel specimens gave an average yield strength for the web of 51.4 k.s.i. and for the flange 59.2 k.s.i.

The joist for Beam IV was to be fully composite and thus had a bottom chord larger than the top chord. The top and bottom chords were $2L^S$ 3 x 2-1/2 x 1/4 long legs back to back and $2L^S$ 3-1/2 x 2-1/2 x 1/4 short legs back to back respectively. The joist for Beam V which was to be tested almost non-composite had the top chord larger than the bottom chord and these were $2L^S$ 3-1/2 x 2-1/2 x 5/16 long legs back to back and $2L^S$ 3-1/2 x 2-1/2 x 1/4 short legs back to back respectively.

Fig. 3.11 shows an elevation and sections of the York Steel joists.

3.2.1 BEAM IV

Beam IV was provided with the required number of shear connectors to achieve its ultimate flexural capacity (13 studs in each shear span).

The connectors were 3/4 in. diameter Nelson studs 3 in. long, with 3 of them placed between each two consecutive panel points.

The joist was instrumented with 44 strain gauges. The concrete slab had 7 filament gauges.

Deflection was recorded at mid-span.

Two dial gauges for slip were placed at the two ends and 3 others at mid-distance on the 3 top chord panels next

to the east support.

Connector and gauge locations are shown on Fig. 3.11. The deflection due to D.L. was 1.5 in. and the maximum compressive strains in the top chord were around 500×10^{-6} in./in. prior to the start of loading.

The load was applied by 1.0 kip increments. The load remained steady up to a load of 20 kips when it started dropping amounts of 0.2 kips.

The load deflection relationship remained linear up to a load of 22.0 kips and then deviated, to become almost horizontal at a load of 38.0 kips. When the beam failed it had deflected 18 in. during the test (Fig. 3.14).

The slip readings were smallest at the east support through most of the testing. Readings were always larger at the locations on the top chord panels and maximum at the second panel from the east support. The load-slip curve was steep up to a load of 27 kips and then the slip increments became large and the curve became almost horizontal. At failure the total end slip was 700×10^{-6} in. The steel strain in the bottom chord followed a straight line relationship with load and started rounding at a test load of 35 kips to reach a plateau at 40 kips. The bottom chord reached its theoretical yield value first under the load points at 30 kips and most of the central region of the bottom chord had yielded at a load of 37 kips.

The concrete strains increased very slowly and at the

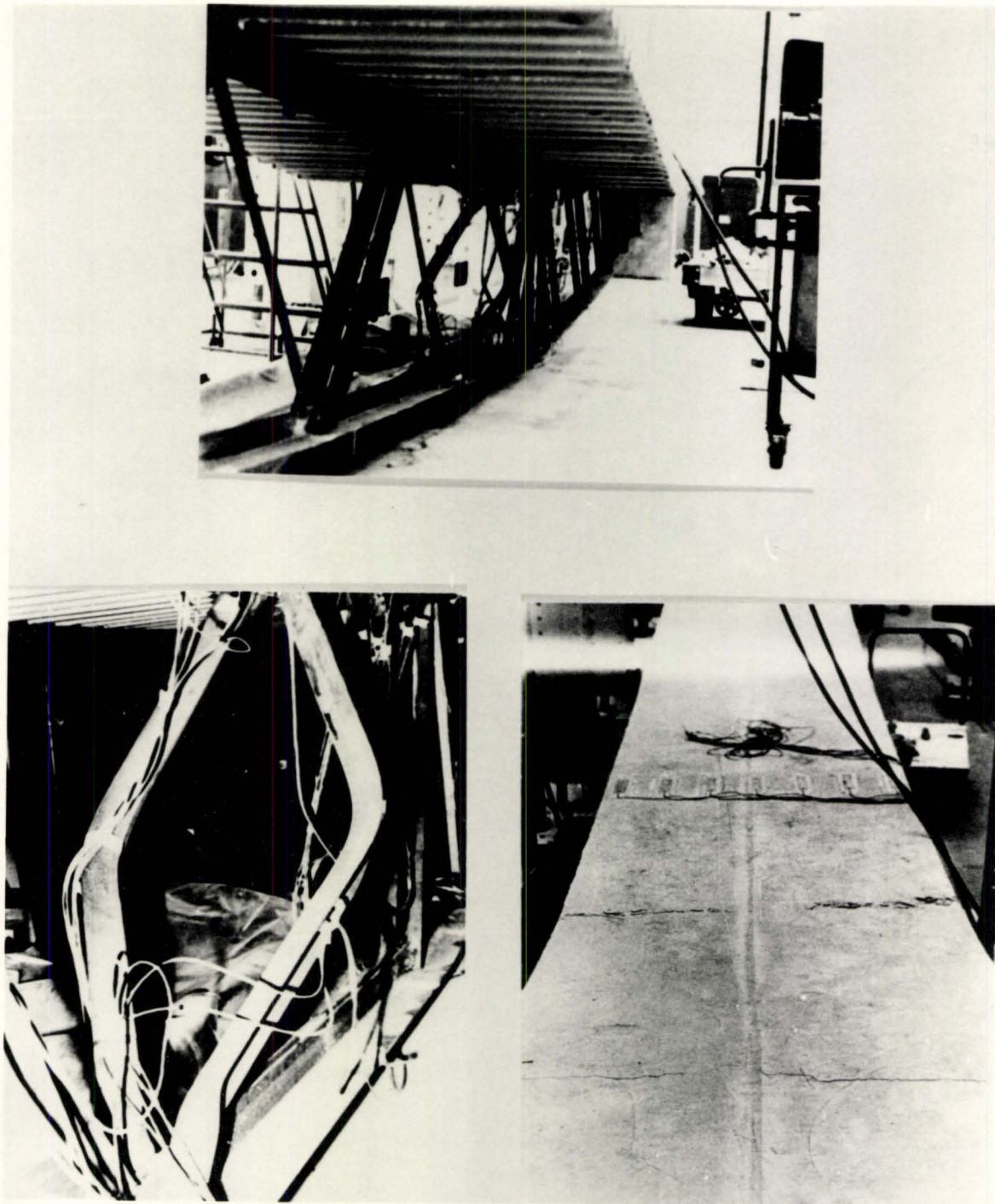


FIG. 3.12 FAILURE OF BEAM IV

same rate in all locations up to 34 kips and then the rate increased considerably. At 36.4 kips a transverse crack appeared along the top of the slab at a distance of 3 ft. 6 in. from the east support and 3/4 in. way down the solid slab. There was also evidence of studs punching through the metal decking in the shear span outside the east load point.

At a load of 43.0 kips the beam had to be unloaded because the bottom chord hit the floor and the supports were raised. When the load was applied again a transverse crack appeared 7 ft. from the east end. With further load increase, the cracks closed up at a load of 40 kips.

The beam failed by buckling of the compression diagonal member below the east load point at a load of 44.6 kips.

Failure is shown in Fig. 3.12.

3.2.2 BEAM V

The shear connection was provided in Beam V by puddle welding the metal decking to the top chord of the joist. One puddle weld was placed at alternate ribs giving a total of 52 welds in the beam.

The steel joist had 44 strain gauges and the concrete slab 7. Deflection was measured at mid-span and at the 2 adjoining panel points on the bottom chord. Two slip gauges were placed at the ends and three along the joist. Connector and gauge locations are shown in Fig. 3.13. Deflection under dead load was 0.85 in.

At mid-span the compressive strain in the top chord was 235×10^{-6} in./in. and the tensile strain in the bottom chord was 300×10^{-6} in./in.

Load was applied in increments of 2.0 kips up to a load of 26 kips and from then on the testing proceeded by adding deflection increments of 0.5 in. each.

Deflections increased elastically up to a load of 21 kips. The curve then rounded and reached a plateau at a load of 27 kips. At failure the specimen had deflected 11.5 in.

The slip readings were larger at the east support and smaller at the west support through most of the test. At failure the maximum slip measured was at the gauge located at 2 ft. 6 in. from the east support and was equal to 0.17 in.

The steel strains in the bottom chord followed a straight line relationship with load up to 31 kips and then reached a plateau. At failure strains were equal to 3900×10^{-6} in./in.

In the top chord the compressive strains decreased from their value at dead load to a low of 180×10^{-6} in./in. at a load of 14 kips, and then increased again all the way up to failure.

The visual signs of failure started when small vertical tension cracks appeared in the solid part of the slab at the upper corner of the ribs just outside the east load point at a load of 30 kips. The deck lifted in the east shear span

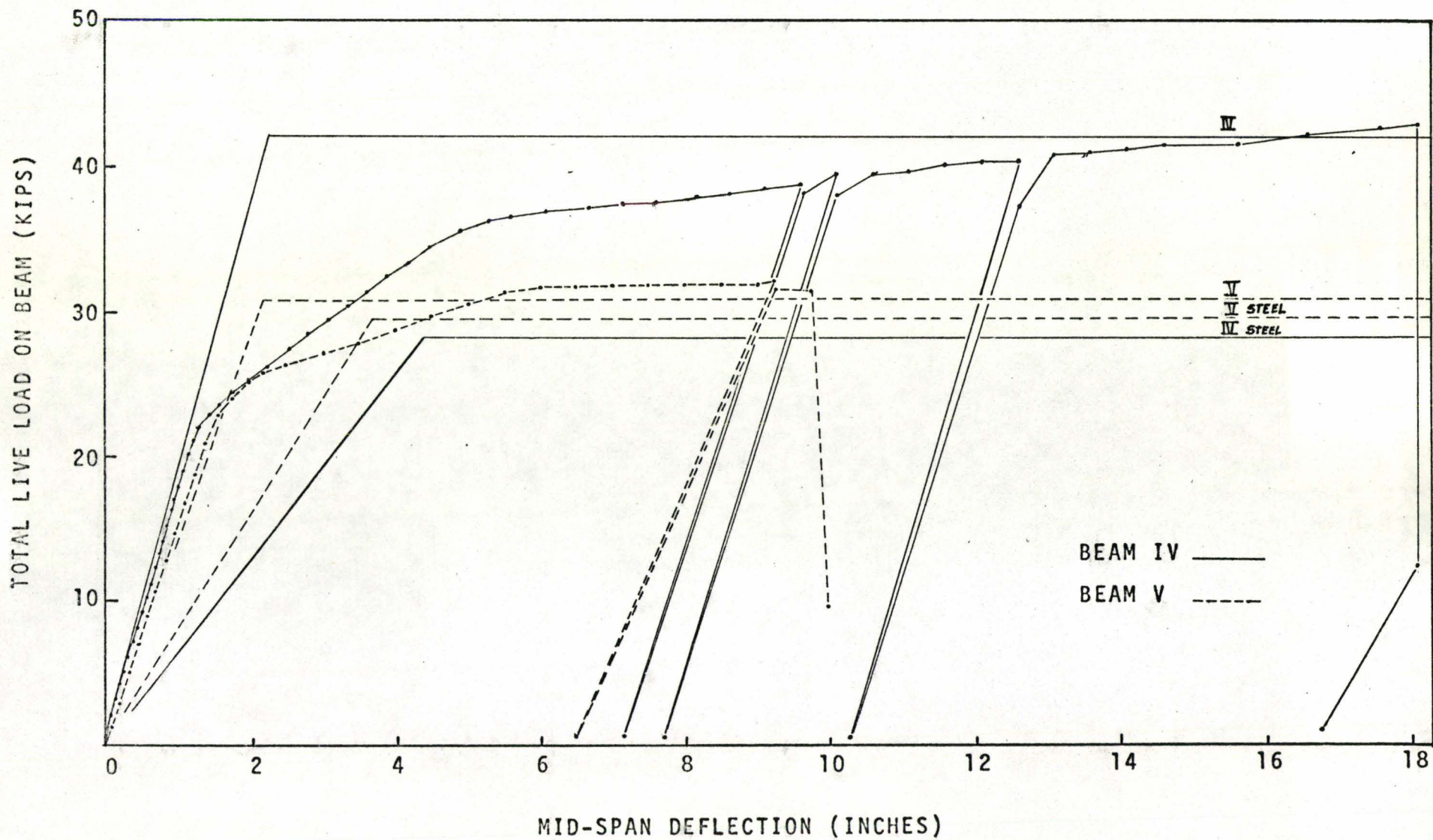


FIG. 3.14 LOAD-DEFLECTION (YORK STEEL JOISTS)

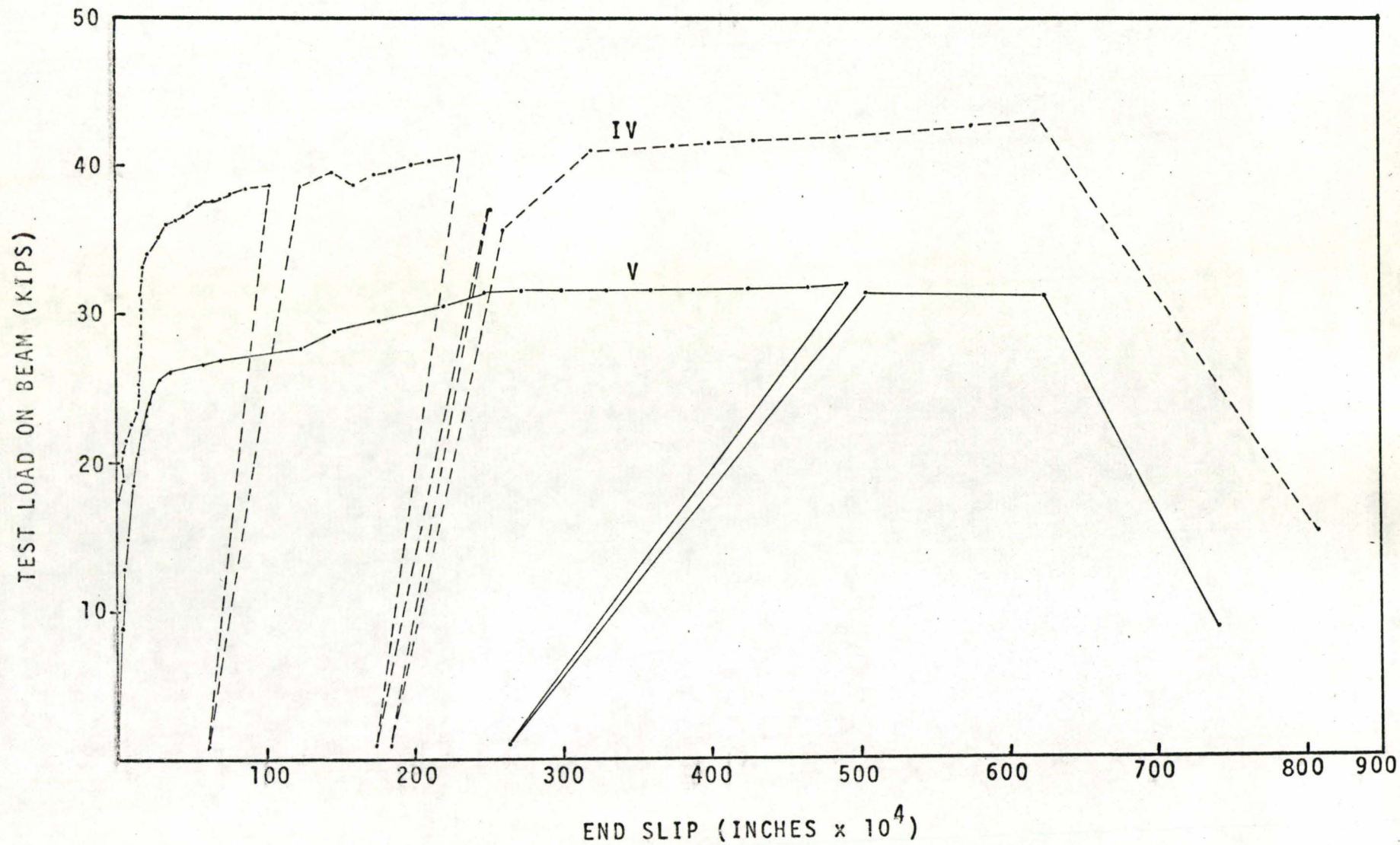


FIG. 3.15 LOAD VERSUS END SLIP (BEAMS IV AND V)

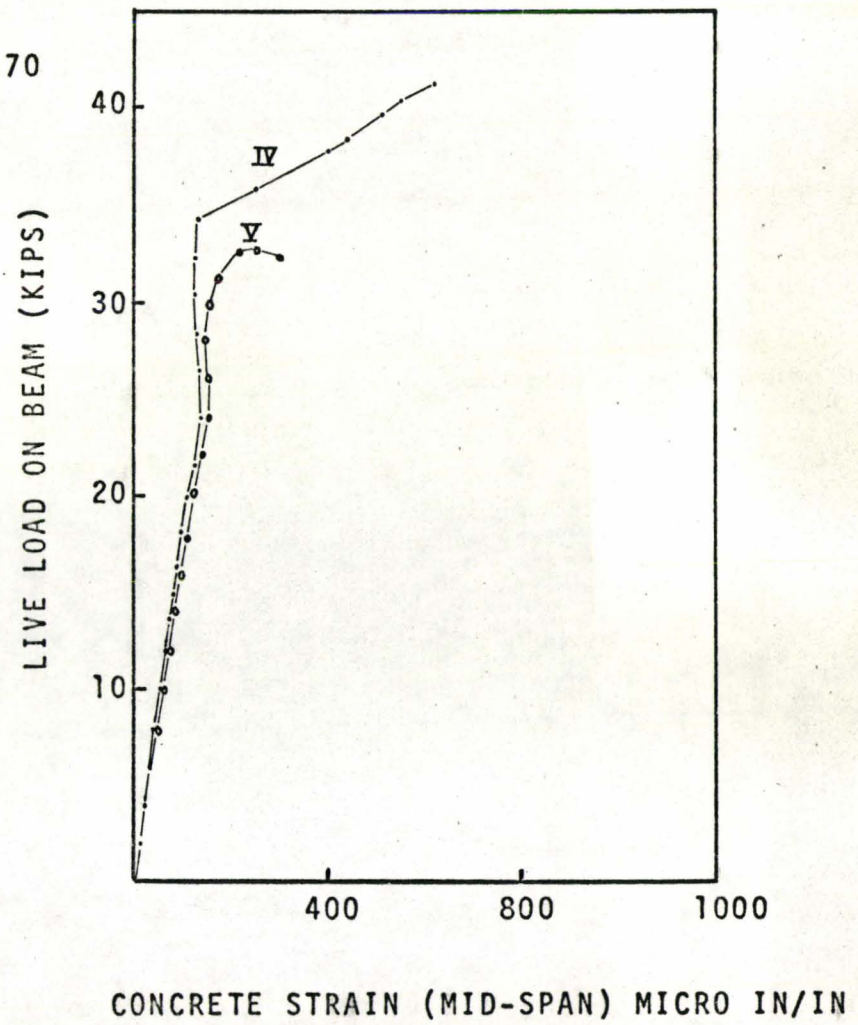
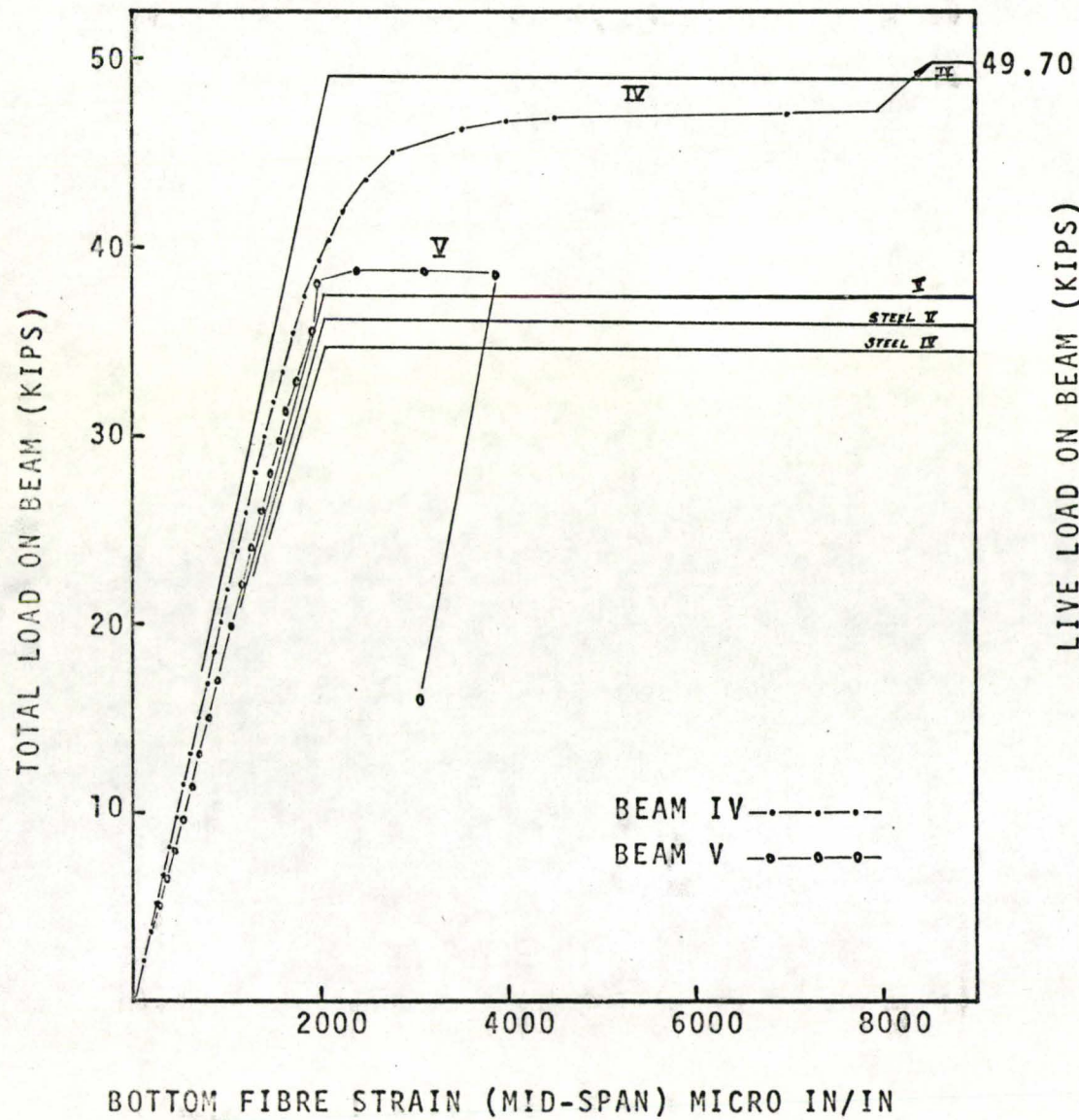


FIG. 3.16 LOAD VERSUS STEEL AND CONCRETE STRAINS (YORK STEEL JOISTS)

at 31.7K and cracks similar to the ones mentioned above appeared just outside the west load point.

At the next application of load ribs started bulging at the interface in the east shear span. After adding another half in, deflection in the cracks increased and extended right through the slab outside the east load point and a tension diagonal next to that point bent out.

When the beam was unloaded because the jack had reached its maximum stroke the cracks opened up along the top on both sides of the load points.

When the load was reapplied and reached 31 kips, the slab pulled away vertically outside both load points. The top of the slab was lower at the east load than at mid-span.

At a load of 31.2K and a total deflection of 11.5 in., the specimen failed by buckling of the top chord outside the east load point.

3.3 G.W.S. JOIST

A Great West Steel joist was used for Beam VI. The top and bottom chords were hat shaped and the web members were tubes.

The joist was made of hot rolled steel and the yield stress obtained from tensile tests was 60 k.s.i.

The top and bottom chords were type J and K, of the shallow hat sections respectively.

The shear connection was achieved in this specimen

by puddle welding the metal decking to the joist top chord. Each rib received two puddle welds, one on each flange of the hat section, giving 200 welds in the beam.

The steel strains were recorded by 22 strain gauges and the concrete slab had 6 filament strain gauges.

An elevation and sections of the beam with weld and gauge locations is shown in Fig. 3.17. Deflections were measured at mid-span and under the load points and slip gauges were placed at the two ends.

Load was applied by one kip increments up to 10 kips and from then on till first yield by 2 kip increments.

Load started dropping amounts of 0.4 kip at a load of 20 kips and at a load of 23 kips, testing proceeded by deflection increments of 1 in. Deflections were elastic till a load of 21 kips and amounted to 3 in. when they reached a plateau. When the beam had deflected 16 in., the bottom chord reached the floor and the specimen was unloaded to lift the supports. At failure the total deflection at mid-span had reached 19.6 in. (Fig. 3.18).

Slip readings were relatively small and slip gauges were removed at a load of 22 kips, at which time the slip at the west end was larger than that at the east end.

Steel strains in the bottom chord behaved elastically from a value of 500×10^{-6} in./in. under dead load to a value of 2100×10^{-6} in./in. at a load of 22 kips, when the bottom chord yielded and strains jumped to a value of 9000×10^{-6}

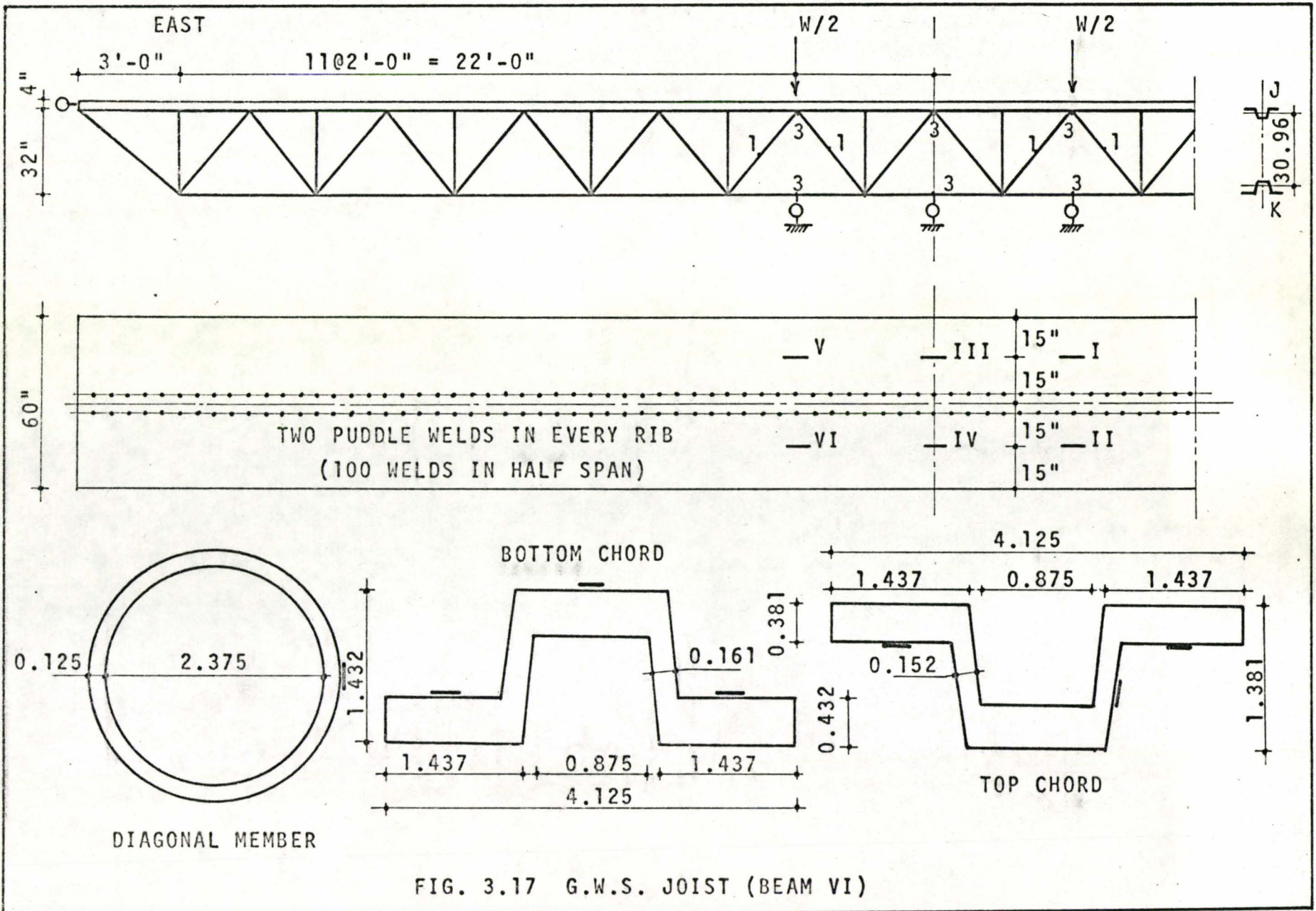


FIG. 3.17 G.W.S. JOIST (BEAM VI)

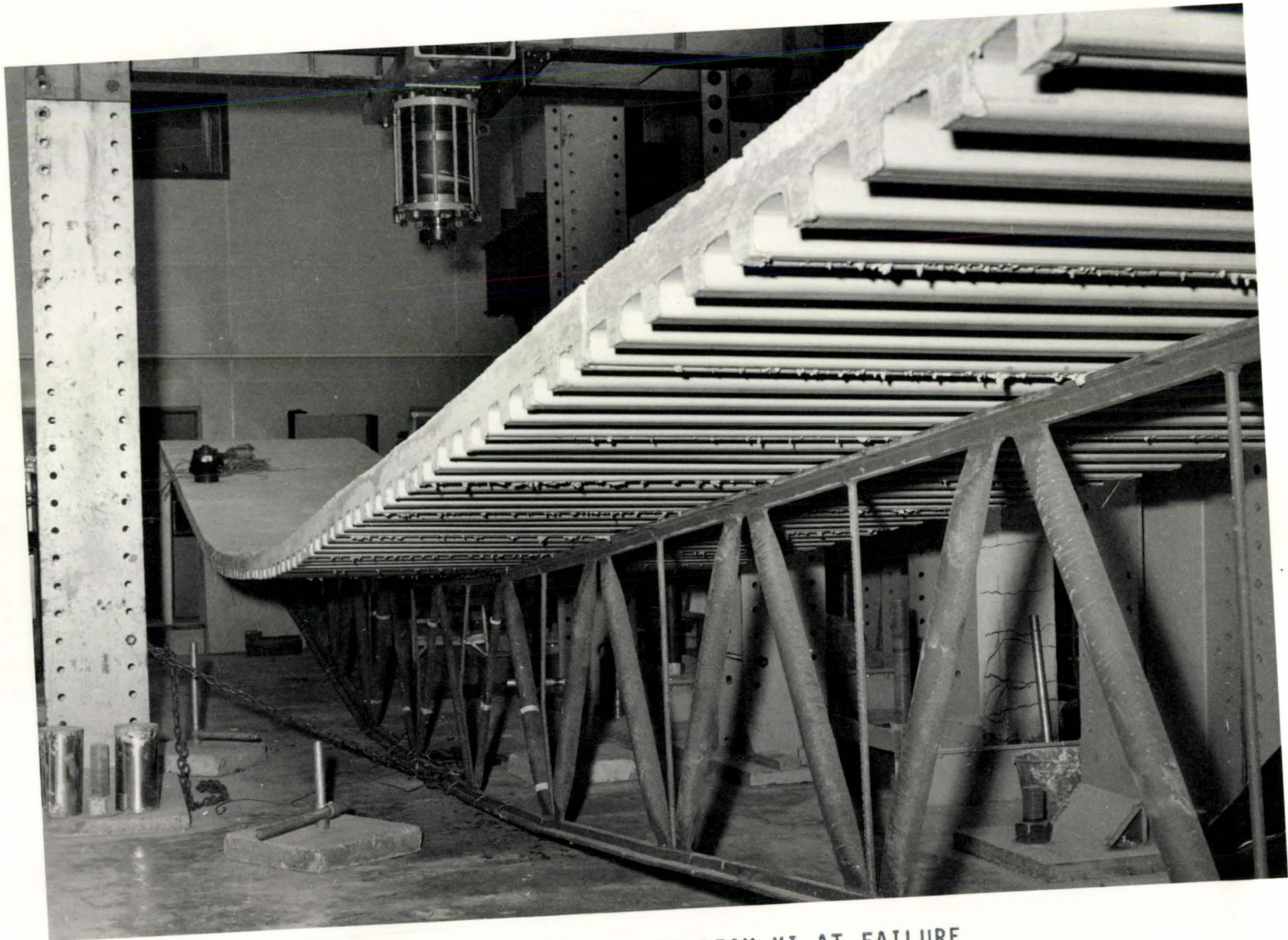


FIG. 3.18 DEFLECTION OF BEAM VI AT FAILURE

in./in. At failure the strains in the bottom chord were $30,000 \times 10^{-6}$ in./in.

The top chord compressive strains decreased from a value of 200×10^{-6} in./in. under dead load to go into tension at a load of 20 kips. The tension increased elastically in the top chord up to a load of 30 kips when they reached a value of 2000×10^{-6} in./in. in the flanges and the top chord yielded.

Concrete strains increased at a steady rate and then jumped when the bottom chord yielded. At failure concrete strains under the load point had reached 2500×10^{-6} in./in. At a load of 31 kips and a deflection of 19.6 in., the specimen failed by fracture of the bottom chord under the east load point (Fig. 3.19).

No cracks appeared in the concrete at any stage of the testing and no connection failure was observed, even after failure.

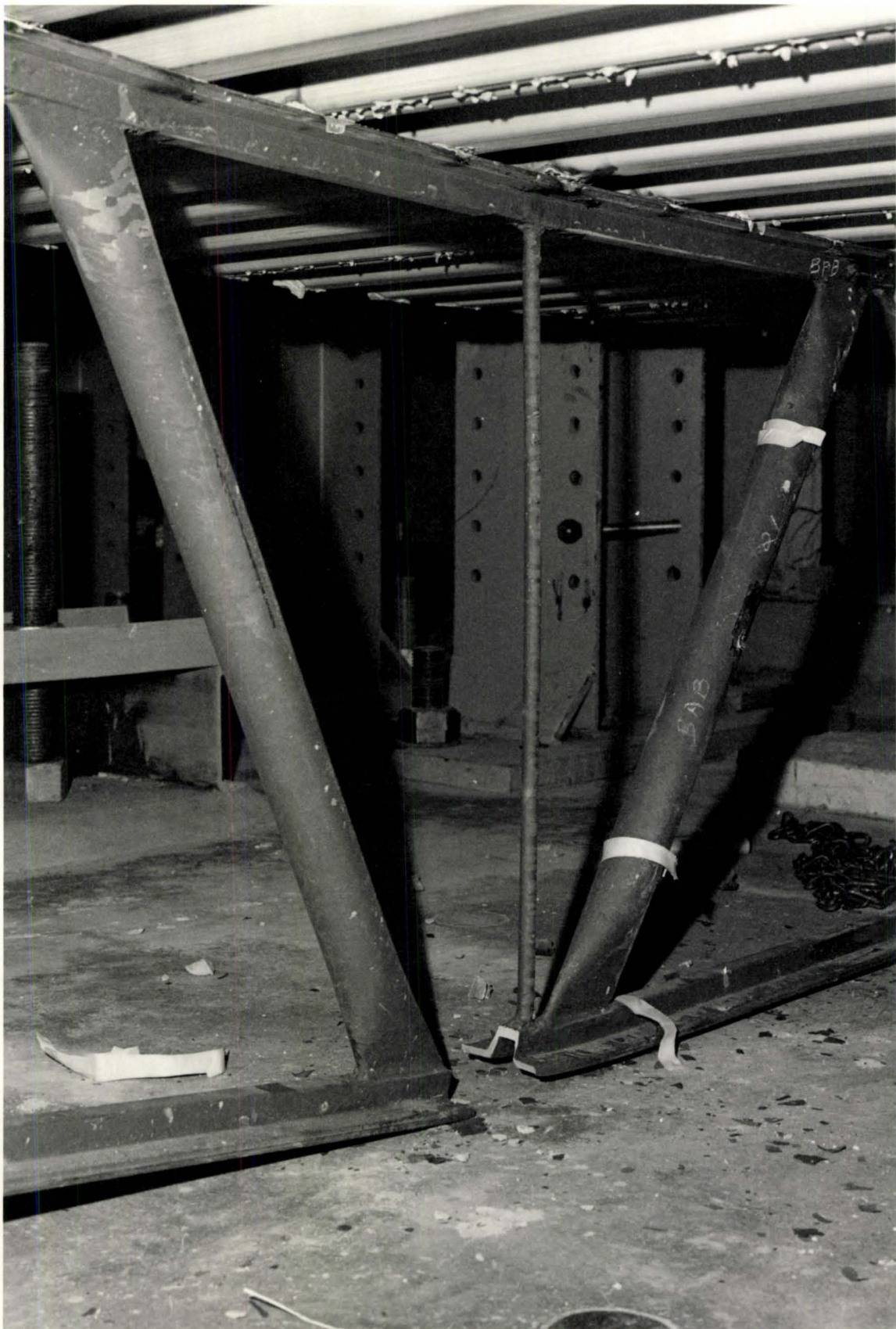


FIG. 3.19 FAILURE OF BEAM VI

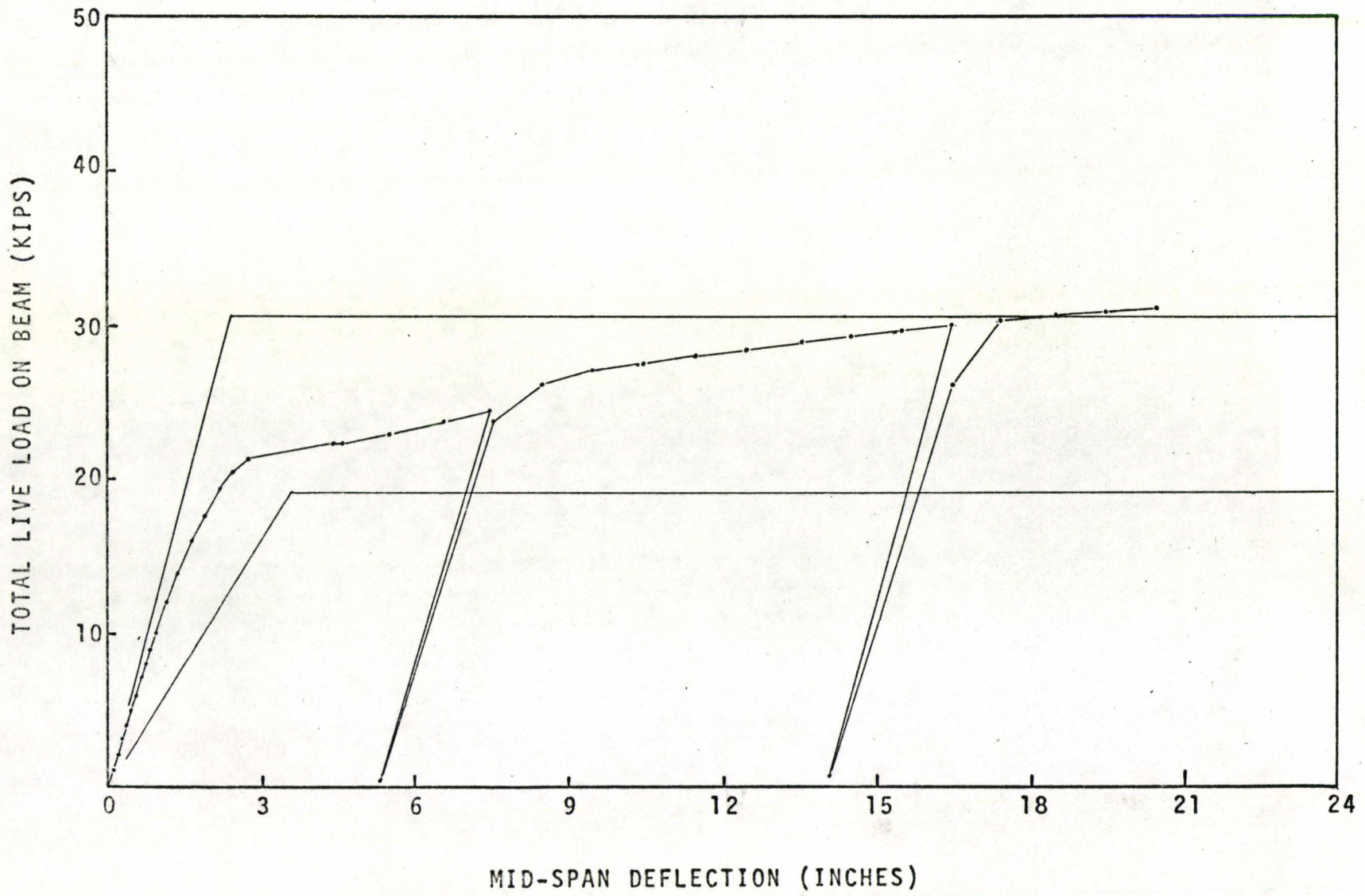


FIG. 3.20 LOAD-DEFLECTION (BEAM VI)

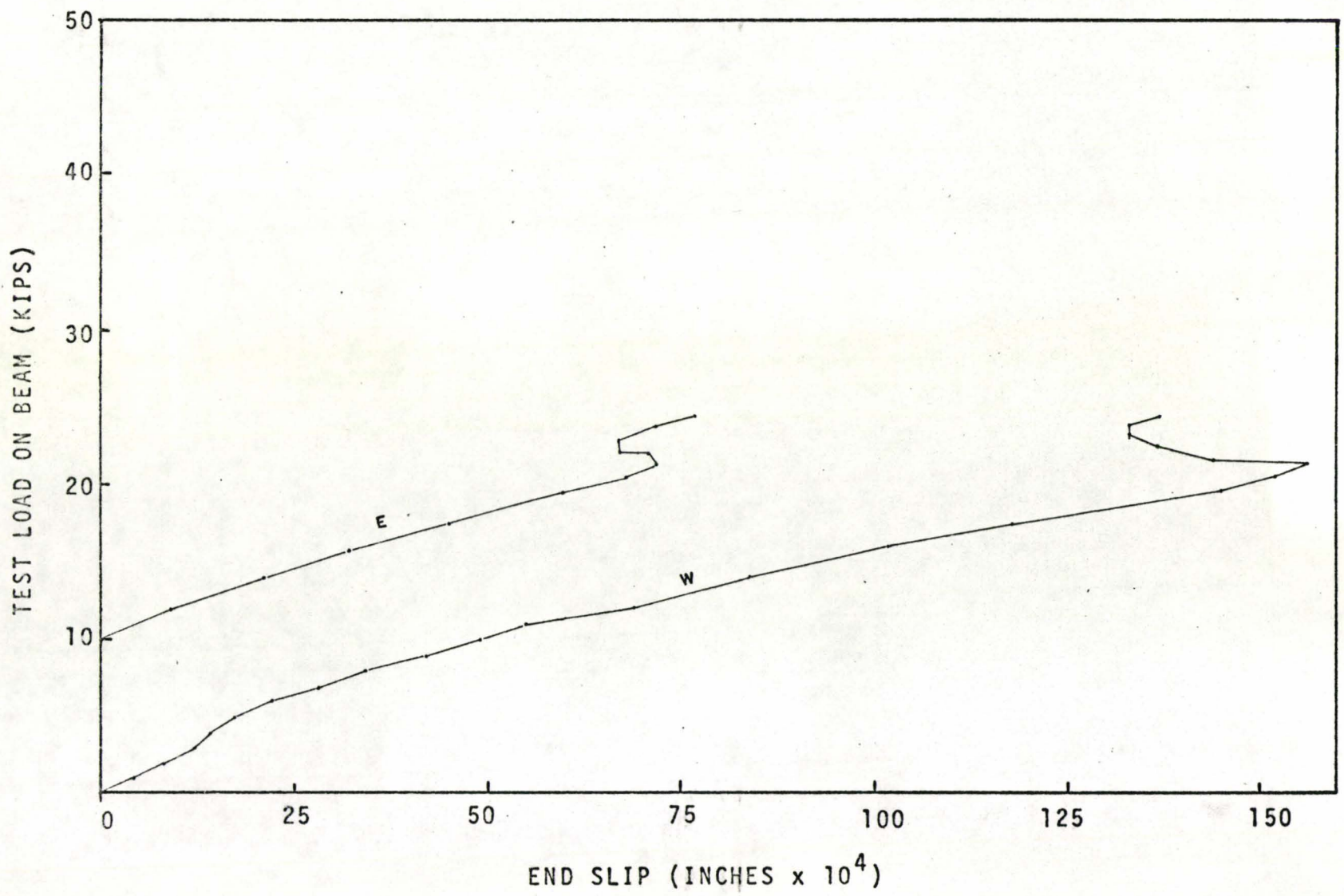


FIG. 3.21 LOAD VERSUS END SLIP (BEAM VI)

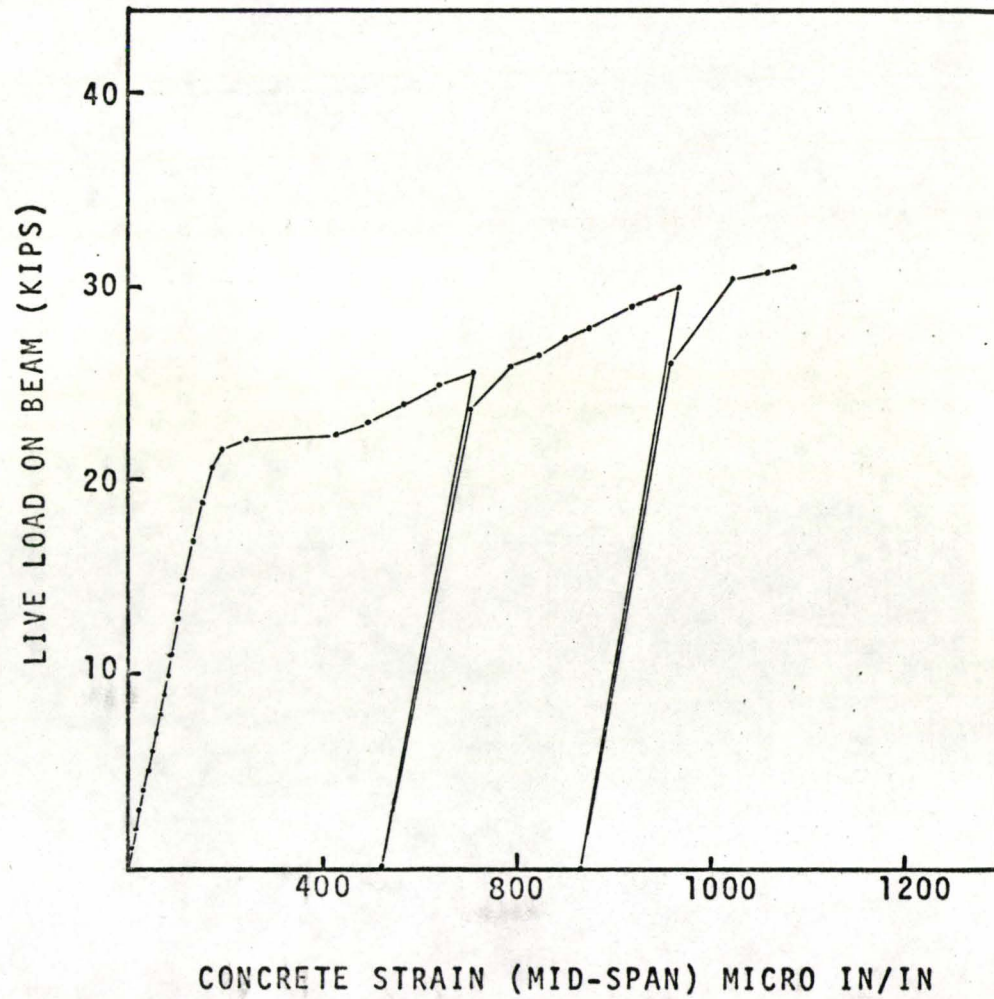
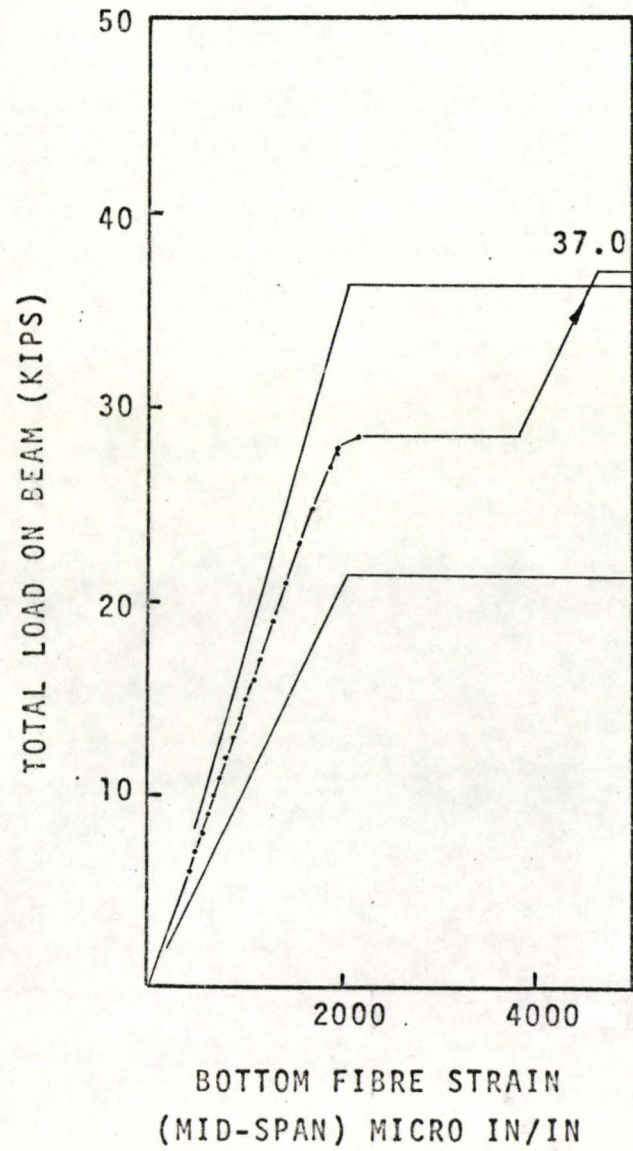


FIG. 3.22 LOAD VERSUS STEEL AND CONCRETE STRAINS (BEAM VI)

CHAPTER IV

ANALYSIS OF RESULTS

4.1 THEORETICAL ANALYSIS

Theoretical approaches to predict stresses and deflections in composite beams have been developed by different researchers (sec. 1.2).

This chapter describes the adaptation of some of these approaches to composite open-web steel joists with ribbed metal deck.

4.1.1 BEAM THEORY

The simplest and most commonly used method for checking stresses and evaluating deflections in composite beams, and the one mentioned in the North American Standards^(11,12) is the beam theory.

The method consists of computing the section properties of the composite joist according to elastic theory by considering the effective area of the concrete in compression as an equivalent area of steel. This is done by dividing the concrete area by the appropriate modular ratio (the ratio of the modulus of elasticity of the steel to that of concrete).

The moment of inertia calculated can then be used in the classical elastic formula $\sigma = \frac{My}{I}$ to calculate stresses, and in the elastic deflection formula to compute the elastic de-

flection. The deflection is increased by 10% to account for the shear deformation effect.

The above mentioned method can be directly applied to fully composite sections.

For the case of partially composite beams the code⁽¹¹⁾ specifies that if fewer than the number of shear connectors required for full composite action are to be provided, the effective area of concrete in compression to be assumed in design is to be reduced in proportion to the ratio of the number of shear connectors provided to the number required for full composite action.

If the ratio is less than one half, no composite action is to be assumed in computing load - carrying capacity and if the ratio is less than one quarter, no composite action is to be assumed for deflection calculations.

The beam theory calculations were used for all test specimens. The modular ratio for each beam was calculated using a modulus of elasticity of 29×10^3 k.s.i. for the steel while the modulus of elasticity for the concrete was calculated from the cylinder test results and the following equation:

$$E_c = 57,000 \sqrt{f'_c} \quad (13)$$

For the beams with full composite action the total area of concrete was used (total width of slab used x thickness of solid part; see 5.1).

For the beams with partial interaction the number of connectors required for full composite action was calculated

BEAM	I	II	III	IV	V	VI
$F_y (K/in^2)$	60.70	60.70	60.70	59.20	59.20	60.00
N_u	29	29	34	16	80	23
N	29	15	42	13	20	42
N/N_u	1.00	0.50	0.50	0.80	0.25	1.00
$Y_{full} (in)$	30.00	30.45	30.09	30.55	30.39	31.70
$Y_{code} (in)$	30.00	27.56	27.25	29.77	24.73	31.70
$Y_{steel} (in)$	19.23	19.23	19.23	16.86	17.36	16.90
$I_{full} (in^4)$	2792	2831	2805	2953	2849	2174
$I_{code} (in^4)$	2792	2526	2497	2862	2230	2174
$I_{steel} (in^4)$	1000	1000	1000	1280	1436	898
$M_{full} (in.K)$	5650	5642	5660	5722	5551	4115
$M_{code} (in.K)$	5650	5562	5563	5690	5338	4115
$M_{steel} (in.K)$	3156	3156	3156	4494	4896	3188

TABLE 5 SECTION PROPERTIES FROM BEAM THEORY

from ultimate design considerations (as suggested in the code) using the ultimate connector strength calculated in sec. 5.1). The number of connectors provided in the beam was divided by the number required for full composite action and the effective concrete area was reduced by this ratio for section property calculations.

The section properties calculated using this theory are shown in Table 5.

4.1.2 FINITE ELEMENT ANALYSIS

Analysing a truss by treating it as a beam is a generally accepted approximation, especially when the member's inertias are relatively small and approximately equal.

But when the moment of inertia of the top chord increases considerably relative to the other members due to the slab acting with it, the treatment of the truss as a beam might lead to some inaccuracy due to the presence of secondary moments, especially in the top chord.

A finite element analysis was thought to be more accurate and was carried out on all test beams.

An available program for the analysis of plane frame structures with joint releases was used. The program operates on a direct assembly stiffness basis, all stiffness coefficients being obtained from a linear analysis of idealized, straight, prismatic members.

A joint is considered to exist at each point of load

application and at points of geometric discontinuity. Loads are permitted only at joints and must have discrete values.

4.1.3 INCOMPLETE INTERACTION THEORY

To calculate the stresses in a composite beam using the elastic theory it is assumed that the strain varies linearly along the cross-section. This is not the case in the beams under investigation as the slip readings, even in the elastic zone cannot be neglected.

The slip produces a strain discontinuity and therefore a theory which takes into consideration the effect of slip has to be used.

The incomplete interaction equation was derived by Newmark, Siess and Viest⁽¹⁾ for beams and later adapted to open-web joists by Galambos and Tide⁽³⁾. The assumptions made in deriving the equation were:

- 1) The shear connection between slab and joist is continuous.
- 2) The change in slip is directly proportional to the change in the connecting force. The constant of proportionality is $1/K$ where K is called the connection shear modulus.
- 3) The curvature of slab and joist is equal at any section.
- 4) All components are elastic and the strain distribution across the section is linear.

EQUILIBRIUM EQUATIONS:

$$\Sigma x = 0 \quad F_c + F_{st} - F_{sb} = 0 \quad (1)$$

$$\Sigma M = 0 \quad F_{sb} \cdot d + F_c \left(G_t + t_r + \frac{t_s}{2} \right) + M_c = M_x \quad (2)$$

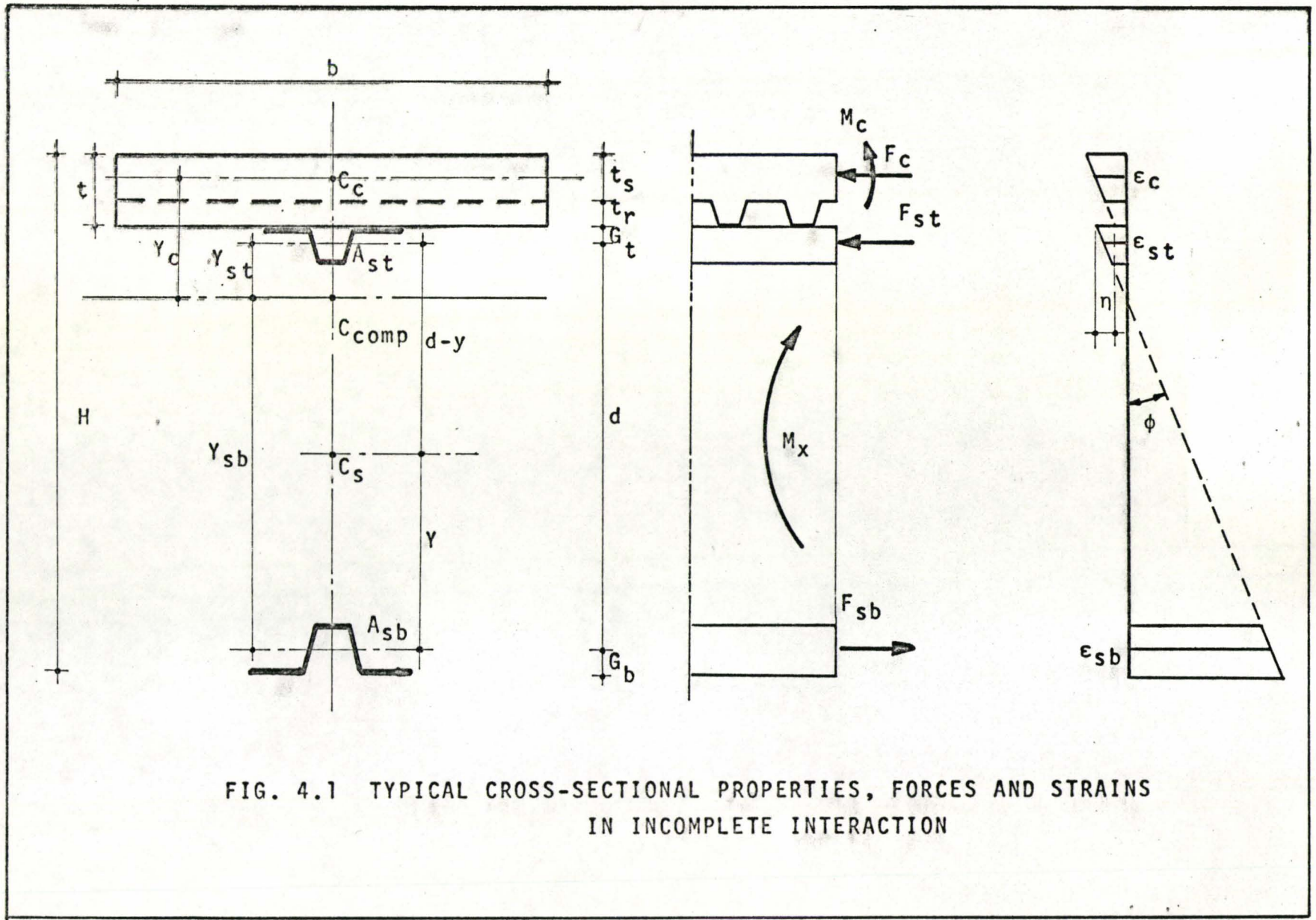


FIG. 4.1 TYPICAL CROSS-SECTIONAL PROPERTIES, FORCES AND STRAINS IN INCOMPLETE INTERACTION

COMPATIBILITY EQUATIONS:

From assumption 3, curvatures are equal at the interface.

$$\phi = \frac{M_c}{E_c I_c} = \left(\frac{F_{st}}{A_{st} E_s} + \frac{F_{sb}}{A_{sb} E_s} \right) \cdot \frac{1}{d}$$

$$\frac{F_{st}}{A_{st}} + \frac{F_{sb}}{A_{sb}} = \frac{ndMc}{I_c} \quad (3)$$

From assumption 4, the strain compatibility at the C.G. of the top chord becomes:

$$\frac{F_c}{A_c E_c} - \frac{M_c (G_t + t_r + \frac{t_s}{2})}{I_c E_c} + \eta = \frac{F_{st}}{A_{st} E_s} \quad (4)$$

where $\eta = - \frac{dy}{dx}$

From assumption 2;

$$\gamma = \frac{Q}{K} = \frac{qs}{K} \quad \text{and} \quad q = \frac{dF_c}{dx}$$

$$\therefore \eta = - \frac{S}{K} \frac{dq}{dx} = - \frac{S}{K} \frac{d^2 F_c}{dx^2}$$

Substituting the value of η in equation (4) and eliminating M_c , F_{st} and F_{sb} from the four equations we get:

$$\frac{d^2 F_c}{dx^2} - C_a K/S \cdot F_c = - C_b K/S \cdot M_x$$

$$\text{where } C_a = \frac{1}{A_c E_c} + \frac{(G_t + t_r + \frac{t_s}{2}) [\beta d + (G_t + t_r + \frac{t_s}{2})(\beta + 1)]}{I_c E_c (\alpha + \beta + 1)}$$

$$+ \frac{[d + \alpha(d + G_t + t_r + \frac{t_s}{2})]}{A_s E_s d(\alpha + \beta + 1)}$$

$$\text{and } C_b = \frac{(G_t + t_r + \frac{t_s}{2})(\beta + 1)}{I_c E_c (\alpha + \beta + 1)} + \frac{\alpha}{A_{st} E_s d (\alpha + \beta + 1)}$$

$$\alpha = \frac{n A_{sb} d^2}{I_c} \quad \text{and} \quad \beta = \frac{A_{sb}}{A_{st}}$$

For the load condition of the tests we have:

$$M_x = \frac{Wx}{2} \quad (0 \leq x < u)$$

$$M_x = \frac{Wu}{2} \quad (u \leq x < L/2)$$

and the boundary conditions are

$$\text{at } x = 0 \quad F_c = 0$$

$$\text{at } x = \frac{L}{2} \quad \frac{dF_c}{dx} = 0 \quad (\text{no slip})$$

$$\text{at } x = u \quad F_c (\text{left}) = F_c (\text{right})$$

$$\text{at } x = u \quad \frac{dF_c}{dx} (\text{left}) = \frac{dF_c}{dx} (\text{right})$$

The solution of the 2nd degree D.E. gives:

$$F_c = \frac{W}{2} \cdot \frac{C_b}{C_a} \left[x - \frac{\sinh(vx)}{v} \left(\frac{\cosh(vL/2 - vu)}{\cosh(vL/2)} \right) \right]$$

$$\text{and } q = \frac{W}{2} \cdot \frac{C_b}{C_a} \left[1 - \cosh(vx) \left(\frac{\cosh(vL/2 - vu)}{\cosh(vL/2)} \right) \right]$$

$$\text{where } v = \sqrt{C_a K/S}$$

For complete interaction

$$q' = \frac{W}{2} \frac{C_b}{C_a}$$

$$\frac{q_r}{q} = 1 - \cosh(vx) \left[\frac{\cosh(vL/2 - vu)}{\cosh(vL/2)} \right] \quad (5)$$

$$\text{but } q = \gamma \frac{K}{S}$$

$$\text{and } \frac{q_r}{q} = \gamma \cdot \frac{K}{S} \cdot \frac{C_a}{C_b} \cdot \frac{2}{W} \quad (6)$$

The unknowns in equations (5) and (6) are q/q' , c , W , K and γ .

By feeding in values of w , γ from the test and using an iterative technique we get a curve relating q and γ .

The slope of the curve at each load gives the value of K .

K was calculated at the working load and fed into the equations to calculate strains and deflections for all test beams.

The results are shown in Tables 7 and 8.

4.2 STEEL STRAINS

To compare the predictions of the various theories, the bottom fibre steel strain at mid-span was chosen.

Although the strains under the load points were larger throughout the testing, as the breakdown of interaction is maximum there, they might have been influenced by secondary moments, welding residual stresses and other factors present at a connection of many members, while at mid-span the bottom chord was in pure tension.

Table 6 shows the loads obtained from the beam theory in accordance with the code.

Table 7 shows the measured bottom fibre strain at mid-span at the working live load predicted by the code.

The measured strains for the test beams range from 4 to 11 percent above those predicted by the beam theory, and from 3 to 13 percent above the ones predicted by the incomplete interaction theory.

Fig. 4.2 shows the load-strain curve for all beams in the elastic region. The fully composite and the non-composite curves are also shown. ϵ_y is calculated from the yield stress obtained from the tensile specimens. ϵ_w is at $0.6 \epsilon_y$. Yield and working load are also shown.

In general it can be seen that the measured strains exceed the theoretical ones.

BEAM	I	II	III	IV	V	VI
P_y FULL (K)	43.800	43.740	43.870	47.680	46.260	32.660
P_y CODE (K)	43.800	43.120	43.120	47.420	44.480	32.660
P_y STEEL (K)	24.460	24.460	24.460	37.450	40.800	25.300
P_y EXP. (K)	34.600	33.000	-	39.000	37.200	29.300
P_w CODE (K)	26.280	25.870	25.870	28.450	26.690	19.600
P_w EXP. (K)	24.000	21.700	22.500	26.400	23.700	18.700
P_w EXP./ P_w CODE	0.913	0.839	0.870	0.928	0.890	0.954

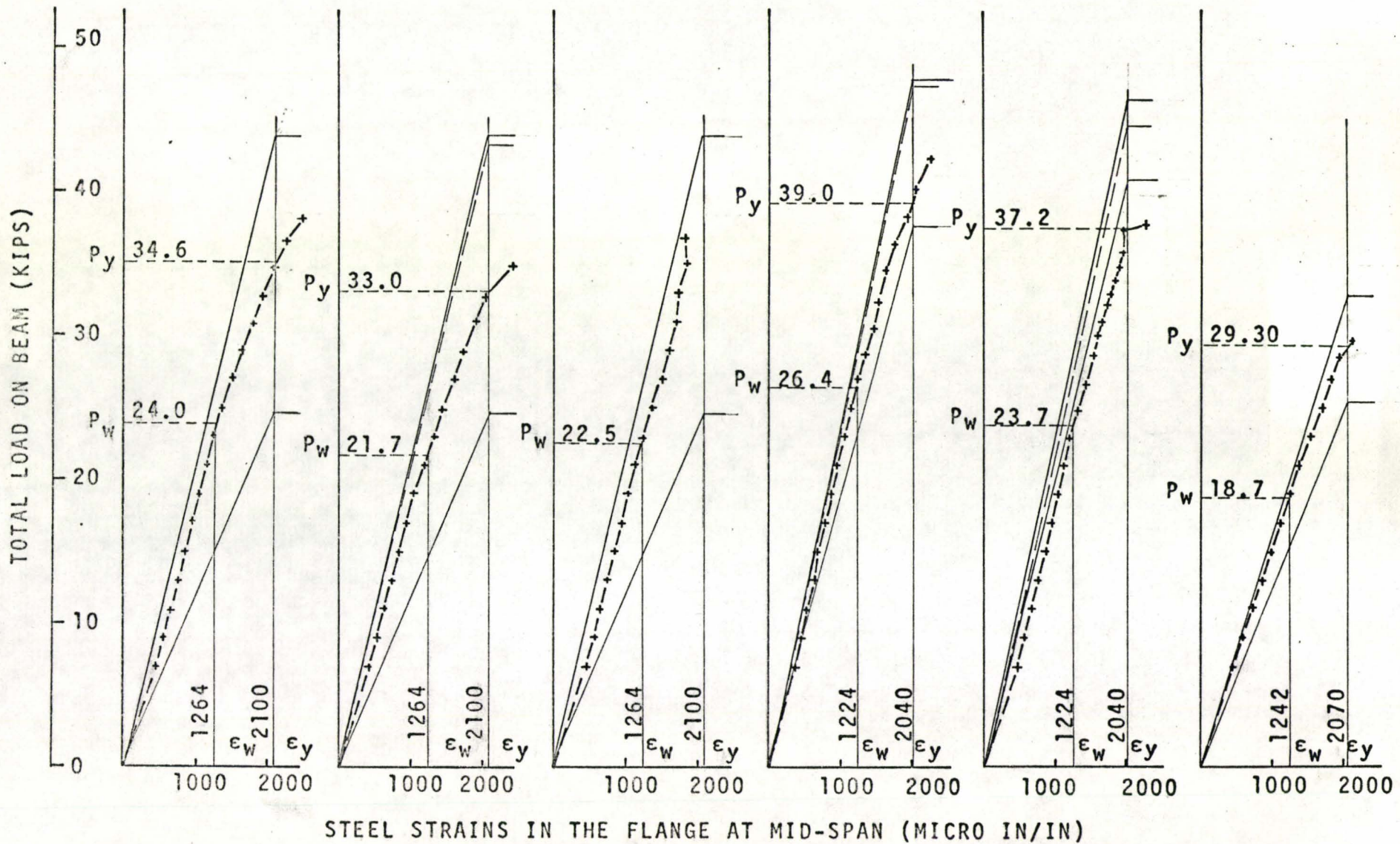
TABLE 6 WORKING LOAD CALCULATIONS (BEAM THEORY)

BEAM	I	II	III	IV	V	VI
Beam Theory *	916	916	916	923	903	797
Incomplete Interaction ‡	922	915	894	934	851	818
Experimental	987	1004	953	959	967	844
$\frac{\text{Experimental}}{\text{Beam Theory}}$	1.076	1.111	1.040	1.038	1.081	1.060
$\frac{\text{Experimental}}{\text{Incomp. Inter.}}$	1.070	1.112	1.068	1.026	1.135	1.032

* Concrete cross-section reduced in accordance with Code

‡ Full concrete cross-section

TABLE 7 BOTTOM FIBRE STRAIN AT MID-SPAN UNDER WORKING LIVE LOAD



4.2 LOAD VERSUS STEEL STRAIN (ALL BEAMS)

4.3 DEFLECTIONS

Deflections were also calculated at mid-span under a live load of P_w computed in accordance with the code. For beam theory calculations the deflection was computed using the deflection expression:

$$\delta = 1.1 \frac{WU}{48EI} (3L^2 - 4U^2)$$

Where the deflection is increased by 10% to account for shear deformation and the moment of inertia used is the one computed according to the code and shown in Table 5.

The finite element program gives deflections directly as an output.

Deflections were calculated from the curvature, forces and moments resulting from the incomplete interaction theory and given as an output together with the strains.

Table 8 shows the deflections calculated by the different methods and compares it with the experimental results.

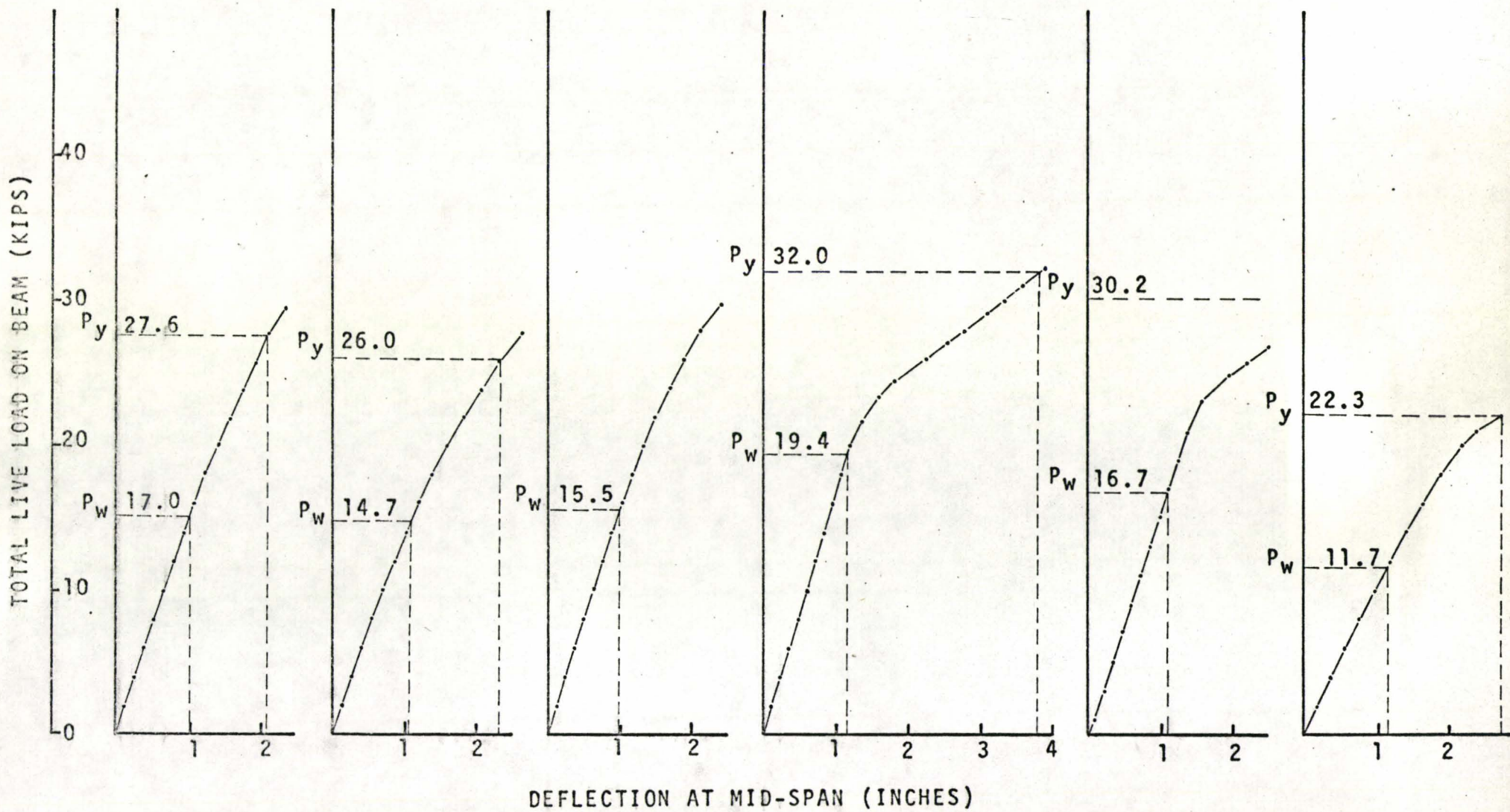
Fig. 4.3 shows the deflection for all test beams in the elastic region. Working and yield loads achieved in tests are shown.

BEAM	I	II	III	IV	V	VI
Beam Theory *	1.203	1.305	1.326	1.208	1.423	0.908
Finite Elements *	1.208	1.314	1.334	1.212	1.424	0.918
Incomplete Interaction ‡	1.100	1.268	1.415	1.095	0.989	0.924
Experimental	1.320	1.470	1.230	1.330	1.290	1.180
<u>Experimental</u> Beam Theory	1.095	1.125	0.928	1.102	0.905	1.298
<u>Experimental</u> Finite Elements	1.092	1.118	0.922	1.096	0.905	1.284
<u>Experimental</u> Incomp. Inter.	1.118	1.159	0.872	1.212	1.303	1.275

* Concrete cross-section reduced in accordance with Code

‡ Full concrete cross-section

TABLE 8 MID-SPAN DEFLECTION AT WORKING LIVE LOAD (INCHES)



4.3 LOAD-DEFLECTION (ALL BEAMS)

CHAPTER V

ULTIMATE STRENGTH DESIGN

5.1 DESIGN PARAMETERS

A first step in determining a design method for a structural system is to evaluate the different parameters affecting the design. Starting from the top down on a section of one of the beams, the parameters to be determined are: the effective slab thickness, the effective slab width and the connector strength.

5.1.1 EFFECTIVE SLAB WIDTH

According to the codes^(11,12) the effective width of slab, in the case of a 50 ft. beam and a slab width of 5 ft. should be equal to the flange width of the top chord plus 16 times the effective slab thickness. This would give an effective slab width of 45 in.

On the other hand test observations and ultimate strength calculations showed that the full 60 in. width of the slab was effective in compression.

To check the effective width experimentally, strain gauges were placed at different distances on the width of the concrete slab at mid-span on test Beam II. Strains recorded at 5, 15 and 25 inches from the slab edge are plotted in Fig. 5.1.

The graph shows concrete strains very close to each other at the 3 locations. This implies that the total width of the slab was effective in compression.

Another indication that the effective slab width was the same as the total slab width in the tests was that when that width was used in the theoretical calculations, the predicted ultimate carrying capacity of the beams agreed well with the experimental ultimate reached.

5.1.2 EFFECTIVE SLAB THICKNESS

The total slab thickness consists of two distinct parts, the solid part above the ribs (2.5 in.) and the ribbed part encased in the metal decking. With the bottom width of the concrete rib being less than 5" and the distance between two ribs larger than one quarter of the total slab thickness, according to the code⁽¹¹⁾ the effective thickness is equal to the depth of the solid part of the slab.

Rotation and cracking of the ribbed part of the slab was observed in some of the tests while the beam was still carrying the applied load, thus indicating that the ribbed part of the slab was not effective in compression.

This was confirmed by the agreement of the theoretical ultimate moment with the experiment when using the solid part of the slab as effective thickness.

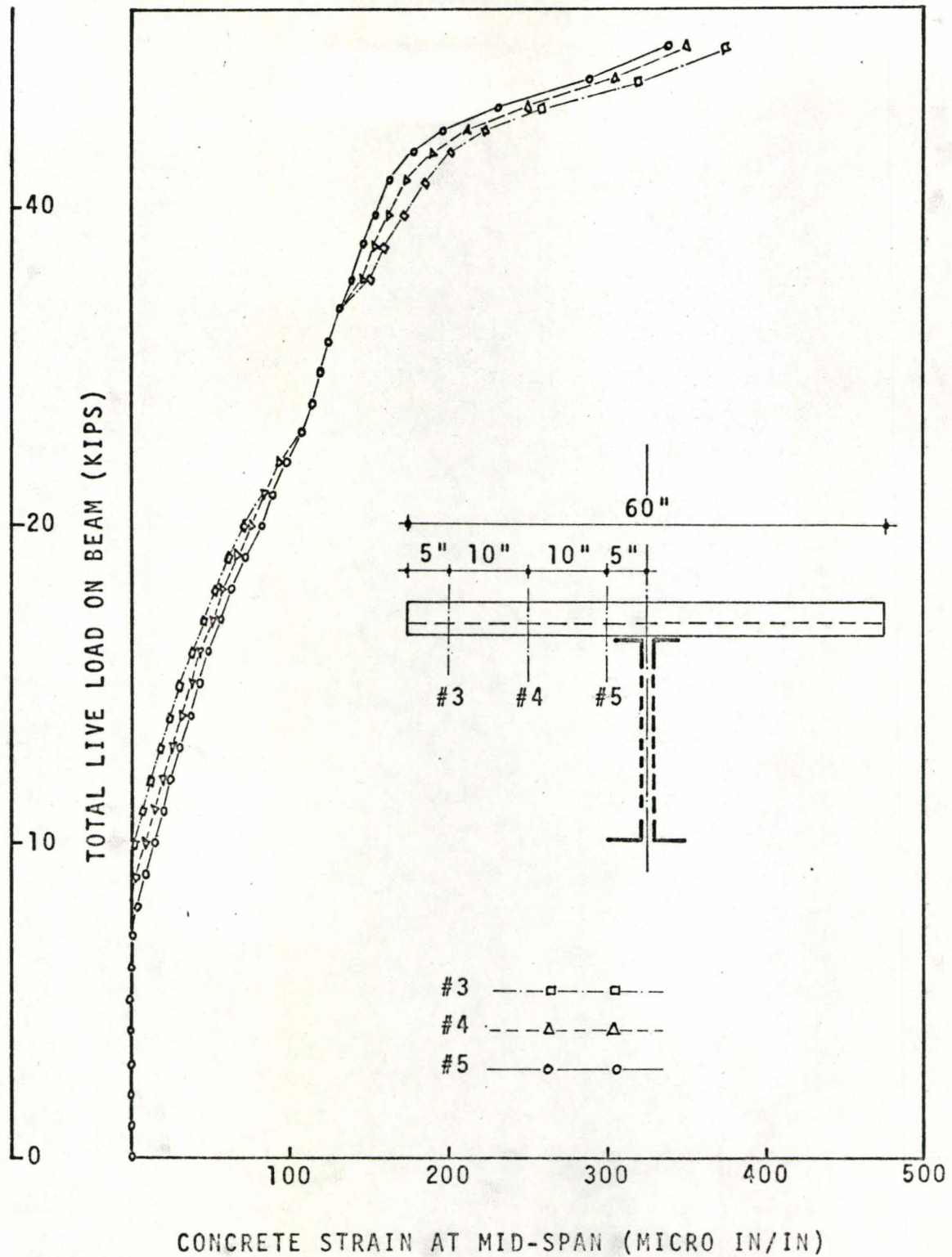


FIG. 5.1 LOAD VERSUS CONCRETE STRAINS (BEAM II)

5.1.3 STRENGTH OF CONNECTORS

Three types of connectors were used in the test specimens.

Three-quarter inch diameter Nelson studs were used in test Beam IV only.

The ultimate strength capacity of this diameter stud had been established in a previous testing program⁽⁹⁾ and was found to be 11.3 kips.

One-half inch diameter Nelson studs were used in test Beams I and II.

Push-out tests performed in a previous testing program⁽¹⁴⁾ had given an ultimate strength of 5.5 kips. The ultimate strength of the 1/2 in. Nelson stud was also calculated from test Beam II which had partial connection, using the buckling load of the top chord as a criteria. These calculations will be detailed below. The ultimate strength obtained was 6.5 kips.

The remaining test beams had puddle welds providing the shear connection and their capacity calculated from test Beam III and checking well with Beam V was found to be 2.1 kips for a single puddle weld.

Beam VI had double puddle welds and although their ultimate capacity was expected to be double of that of the single puddle weld or less, calculations and measured strains showed that they carried 2.5 times as much as a single puddle weld.

This was probably due to the thickness of the flanges

in that joist and to the fact that the welds were done with great care and were protruding about 1/4 in. inside the concrete. This made them stronger than the ones depending only upon the strength of the metal decking.

Calculations For Connectors Strength

One-half In. Nelson Studs (Beam II)

$$M_{\text{actual}} = 5450 \text{ in.K.}$$

$$P_{\text{cr}} \text{ (top chord)} = 67 \text{ K.}$$

$$\text{Moment due to } P_{\text{cr}} \text{ in top chord} = P_{\text{cr}} \times e' = 67 \times 30.01 = 2012 \text{ in.K.}$$

$$\text{Moment due to force in slab} = 5450 - 2012 = 3438 \text{ in.K.}$$

$$C \times e = 3438 \text{ in.K.} \quad (1)$$

$$e = 36 - \left(.96 + \frac{C}{2 \times .85 \times 4.2 \times 60} \right) \quad (2)$$

Solving (1) and (2):

$$C = 97.5 \text{ K.} = Q_u \times 15$$

$$Q_u = 6.5 \text{ kips.}$$

Single Puddle Welds (Beam III)

$$M_{\text{actual}} = 4720 \text{ in.K.}$$

$$P_{\text{cr}} \text{ (top chord)} = 56.5 \text{ K.}$$

$$\text{Moment due to } P_{\text{cr}} \text{ in top chord} = P_{\text{cr}} \times e' = 56.5 \times 30.01 = 1696 \text{ in.K.}$$

$$\text{Moment due to force in slab} = 4720 - 1696 = 3024 \text{ in.K.}$$

$$C \times e = 3024 \text{ in.K.} \quad (3)$$

$$e = 36 - \left(.96 + \frac{C}{2 \times .85 \times 3.7 \times 60} \right) \quad (4)$$

Solving (3) and (4):

$$C = 88.2 \text{ K.} = Q_u \times 42$$

$$Q_u = 2.1 \text{ kips}$$

Double Puddle Welds (Beam VI)

$$M_{\text{actual}} = 4660 \text{ in.K.}$$

$$T_y' \text{ (top chord)} = 105.6 \text{ K.}$$

$$\begin{aligned} \text{Moment due to tension in top chord} &= T_y' \times e' = 105.6 \times 6 \times 30.957 \\ &= 3290 \text{ in.K.} \end{aligned}$$

$$\text{Moment due to force in slab} = 4660 + 3290 = 7950 \text{ in.K.}$$

$$C \times e = 7950 \text{ in.K.} \tag{5}$$

$$e = 36 - (.535 + \frac{C}{2 \times .85 \times 4.8 \times 60}) \tag{6}$$

Solving (5) and (6):

$$C = 225.5 \text{ K.} = Q_u \times 42$$

$$Q_u = 5.36 \text{ kips.}$$

5.2 DESIGN METHOD

The ultimate strength design method is a method based on equilibrium considerations.

While trying to obtain a design procedure based on ultimate strength it has been noticed that there are three possible cases for the section.

Case 1: Balanced Section.

Case 2: Over-Connected Section.

Case 3: Under-Connected Section.

The criteria used to differentiate between the 3 cases is the amount of shear connection provided.

If the total ultimate strength of the connectors in the shear span is equal to the maximum tension that can be developed in the bottom chord, the section is balanced.

If the connectors can carry a force larger than that tension, the section is over-connected; and if there are not enough connectors to achieve a balanced design, the section is under-connected (Fig. 5.2).

CASE 1: BALANCED SECTION:

The connector strength is just enough to create a compression in the concrete equal to the tension in the bottom chord when its stress reaches yield.

The ultimate stress of steel is larger than the yield stress. Ultimate was reached in tests Beam I and VI when the bottom chord fractured, but achieving this type of failure is not guaranteed. Therefore, for safety the yield stress of

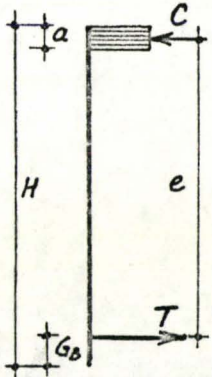
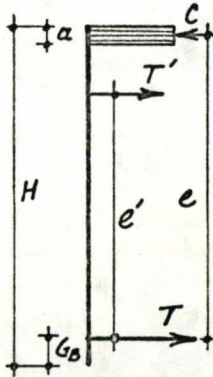
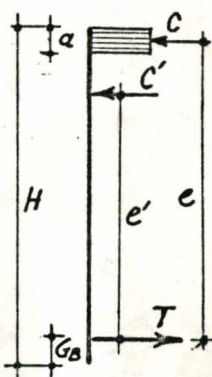
CASE 1 $\Sigma Q_u = A_{sb}F_y$ BALANCED SECTION	CASE 2 $\Sigma Q_u > A_{sb}F_y$ OVER-CONNECTED SECTION	CASE 3 $\Sigma Q_u < A_{sb}F_y$ UNDER-CONNECTED SECTION
<p> $T = A_{sb}F_y$ $C = \Sigma Q_u$ </p>  <p> $a = \frac{C}{0.85 f_c b}$ $e = H - (G_b + \frac{a}{2})$ </p>	<p> $T = A_{sb} \cdot F_y$ </p> <p> (a) $\Sigma Q_u > T + A_{st}F_y$ $C = (A_{sb} + A_{st})F_y$ $T' = A_{st}F_y$ </p> <p> (b) $\Sigma Q_u < T + A_{st}F_y$ $C = \Sigma Q_u$ $T' = C - T$ </p> <p> $a = \frac{C}{0.85 f_c b}$ $e = H - (G_b + \frac{a}{2})$ $e' = H - (G_b + G_t + t)$ </p> 	<p> $C = \Sigma Q_u$ </p> <p> (a) $C + P_{cr} > A_{sb}F_y$ $T = A_{sb}F_y$ $C' = A_{sb}F_y - C$ </p> <p> (b) $C + P_{cr} < A_{sb}F_y$ $C' = P_{cr}$ $T = C + P_{cr}$ </p> <p> $a = \frac{C}{0.85 f_c b}$ $e = H - (G_b + \frac{a}{2})$ $e' = H - (G_b + G_t + t)$ </p> 
$M_{ult} = C \times e$	$M_{ult} = C \times e - T' \times e'$	$M_{ult} = C \times e + C' \times e'$

TABLE 9 ULTIMATE STRENGTH DESIGN

the steel shall be used in the design. The tension in the bottom chord acts at the centre of gravity.

The compression in the concrete slab acts at the centroid of the stress block with a compressive stress of $0.85 f'_c$.

The ultimate moment of the section is the product of either the tension or the compression multiplied by the distance between them.

CASE 2: OVER-CONNECTED SECTION:

The combined carrying capacity of the shear connectors is higher than the force developed in the bottom chord when it reaches yield.

The bottom chord continues to yield and the top chord also goes into tension.

The compressive force keeps increasing in the concrete slab resulting in more tension in the top chord to keep the section in equilibrium, because the force in the bottom chord is constant at a value of $A_{sb} \times F_y$.

There are then two possibilities:

(a) The strength of the connectors is high enough to get the top chord also to yield. The compression in the concrete slab is then equal to the area of both top and bottom chord times the steel yield stress.

Failure usually occurs in the bottom chord as it is improbable that the slab fails in compression because its choice is governed by other considerations which makes it cap-

able of carrying a large amount of compression.

(b) The strength of the connectors is not enough to introduce yielding in the top chord. The compression in the concrete slab is equal to the combined ultimate strength of the connectors. The tension in the top chord is the difference between that compression and the ultimate capacity of the bottom chord.

Failure can occur in the connectors or in the bottom chord.

The ultimate moment for an over-connected section is equal to the compression in the slab acting in the middle of the concrete stress block times its lever arm less the tension in the top chord times the distance between the C.Gs. of top and bottom chords.

The increase in M_{ult} over the balanced section is:

$$\begin{aligned}\Delta M &= M_2 - M_1 \\ &= [(A_{sb} \cdot F_y + T')e_2 - T'e'] - [(A_{sb} \cdot F_y)e_1]\end{aligned}$$

assuming that the difference between e_1 and e_2 is negligible.

$$e_1 = e_2 = e$$

$$\Delta M = T'e - T'e' = T'(e - e')$$

$$T'_{max} = A_{st} \cdot F_y \quad \text{and} \quad (e - e')_{max} = t + G_t$$

$$\therefore \Delta M_{max} = A_{st} \cdot F_y (t + G_t)$$

In all test specimens and in most practical cases $t + G_t$ is around 5 in. Consequently the increase in M_{ult} is not too

large and the designer has to find out if the increase in connector number to create an over-connected section is an economical solution.

CASE 3: UNDER-CONNECTED SECTION:

The total ultimate carrying capacity of the connectors is not enough to get the bottom chord to yield. The top chord has to help by taking some compression. The amount of compressive force the top chord can carry cannot exceed its critical buckling load.

There are two possibilities:

(a) The sum of the compression in the slab and the buckling load for the top chord exceeds $A_{sb} \cdot F_y$. The tension in the bottom chord is then $A_{sb} F_y$ and the difference between that tension and the compression in the concrete goes into the top chord. This compressive force is less than P_{cr} and the top chord does not buckle. Once the bottom chord keeps on yielding, failure usually occurs in the following way:

The connectors fail and all the compressive force is transferred suddenly to the top chord which buckles immediately. Buckling is due to the load increase and also to the buckling length increase if the connectors, which are preventing the top chord from buckling, fail.

(b) Yielding in the bottom chord cannot be reached and the force in the top chord increases until the top chord buckles.

It has to be borne in mind that decreasing the number of connectors and getting an under-connected section has a

two-fold effect on the top chord as both the compressive force in it and its buckling length increase simultaneously.

For an under-connected section the tension in the bottom chord and the compression in the top chord both act at the C.G. of the chords. As for the compression in the concrete, it is also considered to act at the centroid of the ultimate stress block, although it is believed that this point requires further investigation (this will be discussed in the next chapter).

The ultimate moment is equal to the compression in the slab times its lever arm plus the compression in the top chord times its lever arm.

Table 10 shows the calculation of the ultimate moment for all test beams using the ultimate strength method described. The ultimate moment calculated is compared with the experimental one.

Table 11 is the same table except that instead of using F_y obtained from tensile tests, F_{act} measured by the strain gauges or F_{ult} when the bottom chord ruptured are used instead.

BEAM	I	II	III	IV	V	VI
$A_{sb}F_y(K)$	173.00	173.00	173.00	170.50	170.50	120.00
$\Sigma Q_u(K)$	188.00	97.50	88.20	147.00	42.00	226.00
$P_{cr}(K)$	67.00	67.00	56.50	93.00	101.50	58.00
$A_{st}F_y(K)$	111.50	111.50	111.50	155.00	211.00	106.00
Case	2(b)	3(b)	3(b)	3(a)	3(b)	2(a)
T(K)	173.00	164.50	144.70	170.50	143.50	120.00
T'(K)	15.00	-	-	-	-	106.00
C(K)	188.00	97.50	88.20	147.00	42.00	226.00
C'(K)	-	67.00	56.50	23.50	101.50	-
a(in)	1.06	0.46	0.48	0.60	0.22	0.92
e(in)	34.51	34.81	34.80	35.09	35.28	35.00
e'(in)	30.01	30.01	30.01	30.48	30.25	30.96
C x e(in.K)	6480	3385	3070	5160	1480	7900
(C' or -T')xe' (in.K)	-450	2010	1695	716	3070	-3280
M_{ult} (in.K)	6030	5395	4765	5876	4550	4620
M_{exp} (in.K)	6230	5450	4720	5950	4680	4660
M_{exp}/M_{ult}	1.034	1.010	0.991	1.013	1.027	1.010

TABLE 10 ULTIMATE MOMENT CALCULATION FOR TEST BEAMS
USING DESIGN METHOD

BEAM	I	II	III	IV	V	VI
$A_{sb} F_{act} (K)$	188.00	173.00	154.00	170.50	144.00	130.00
$\Sigma Q_u (K)$	188.00	97.50	88.20	147.00	42.00	226.00
$P_{cr} (K)$	67.00	67.00	56.50	93.00	101.50	58.00
$A_{st} F_y (K)$	111.50	111.50	111.50	155.00	211.00	106.00
Case	1	3(b)	3(b)	3(a)	3(b)	2(b)
T(K)	188.00	173.00	154.00	170.50	144.00	130.00
T' (K)	-	-	-	-	-	96.00
C(K)	188.00	97.50	88.20	147.00	42.00	226.00
C' (K)	-	75.50	65.80	23.50	102.00	-
a(in)	1.06	0.46	0.48	0.60	0.22	0.92
e(in)	34.51	34.81	34.80	35.09	35.28	35.00
e'(in)	30.01	30.01	30.01	30.48	30.25	30.96
C x e(in.K)	6480	3385	3070	5160	1480	7900
(C' or -T')xe' (in.K)	-	2265	1974	716	3070	-2970
M _{ult} (in.K)	6480	5650	5044	5876	4550	4930
M _{exp} (in.K)	6230	5450	4720	5950	4680	4660
M _{exp} /M _{ult}	0.965	0.966	0.937	1.013	1.027	0.946

TABLE 11 ULTIMATE MOMENT CALCULATION FOR TEST BEAMS
USING EXPERIMENTAL RESULTS

5.3 LOAD FACTOR

The load factor is defined as the ultimate load divided by the design working load.

Load factors for all test beams are shown in Table 12.

P_{ult} (theoretical) and P_{ult} (experimental) are the ultimate load evaluated by the ultimate design method and the ultimate load achieved in the test.

P_w (code) and P_w (experimental) are the working load at $0.6 F_y$ calculated using the composite moment of inertia according to the code and the total load on the beam when the measured bottom fibre strain was $0.6 F_y$.

For the shear connectors, the load factor is the load on a connector at ultimate moment divided by the load on the connector at working load level.

Load factors for connectors are shown in Table 13.

The load on the connector at working load is computed using incomplete interaction theory. The load shown in the table is the load on the end connector as according to the theory this connector is the mostly stressed.

Another value of q for a fully composite section is shown. $q = \frac{VQ}{I_{comp}}$ where V is the end reaction at working load and Q is the first moment of area of the concrete slab about the center of gravity of the composite section.

The last row of Table 12 has the shape factor for all test beams. It will be noted that the shape factor is less than unity for all beams with incomplete interaction.

BEAM	I	II	III	IV	V	VI
$P_{ult}(\text{theo.})$	46.800	41.800	36.900	49.000	37.900	36.700
$P_{ult}(\text{exp.})$	48.200	42.200	36.600	49.600	39.000	37.000
$P_w(\text{code})$	26.280	25.870	25.870	28.450	26.690	19.600
$P_w(\text{exp.})$	24.000	21.700	22.500	26.400	23.700	18.700
$P_y(\text{code})$	43.800	43.740	43.870	47.420	44.480	32.660
$\frac{P_{ult}(\text{exp.})}{P_w(\text{code})}$	1.834	1.631	1.415	1.743	1.461 (1.755)**	1.979
* $\alpha = \frac{P_{ult}(\text{theo.})}{P_y(\text{theo.})}$	1.068	0.969	0.856	1.033	0.852	1.124

* α = shape factor

** load factor for Beam V when composite action neglected

TABLE 12 LOAD FACTOR FOR BEAMS

BEAM	I	II	III	IV	V	VI
Connector Type	1/2 in.	1/2 in.	Single Puddle Weld	3/4 in.	Single Puddle Weld	Double Puddle Weld
Load on end Con- * tor/in. at P_w (code), Q_u	0.279	0.271	0.273	0.310	0.260	0.184
Shear Span	258	258	258	240	240	252
Number of Connectors	29	15	42	13	26	42
$q = \frac{VQ}{I_{comp}}$	0.279	0.284	0.277	0.311	0.294	0.180
Q_w	2.480	4.660	1.680	5.230	2.400	1.110
Q_{ult}	6.500	6.500	2.100	11.300	2.100	5.360
Q_{ult}/Q_w	2.620	1.390	1.250	2.160	.880	4.830

* computed by incomplete interaction theory

TABLE 13 LOAD FACTOR FOR CONNECTORS

This is because the theoretical yield load computed in accordance with the code P_y (code) is higher than the theoretical ultimate load P_{ult} (theoretical).

The reason P_y (code) is higher than P_{ult} (theoretical) is that in the case of partial connection, the recommended reduction in concrete area takes care of the reduction in number or strength of connectors but does not account for any increase in flexibility of the connectors.

This is clear in Fig. 5.2 where 3 curves are shown. The highest line is for a beam with full interaction where the ultimate load is higher than the yield load and the shape factor is larger than unity.

The middle line is the code line for a beam with partial connection computed by reducing the concrete area and thus the stiffness. This line intersects ϵ_y at a load P_y (code) just below P_y (full).

The lowest line represents the actual behaviour of a beam with incomplete interaction. The increase of flexibility of the beam reduces the slope of the line which intersects ϵ_y at a load P_y (exp.) lower than P_y (code). Although the load increases subsequently to a P_{ult} it does not reach the level of P_y (code).

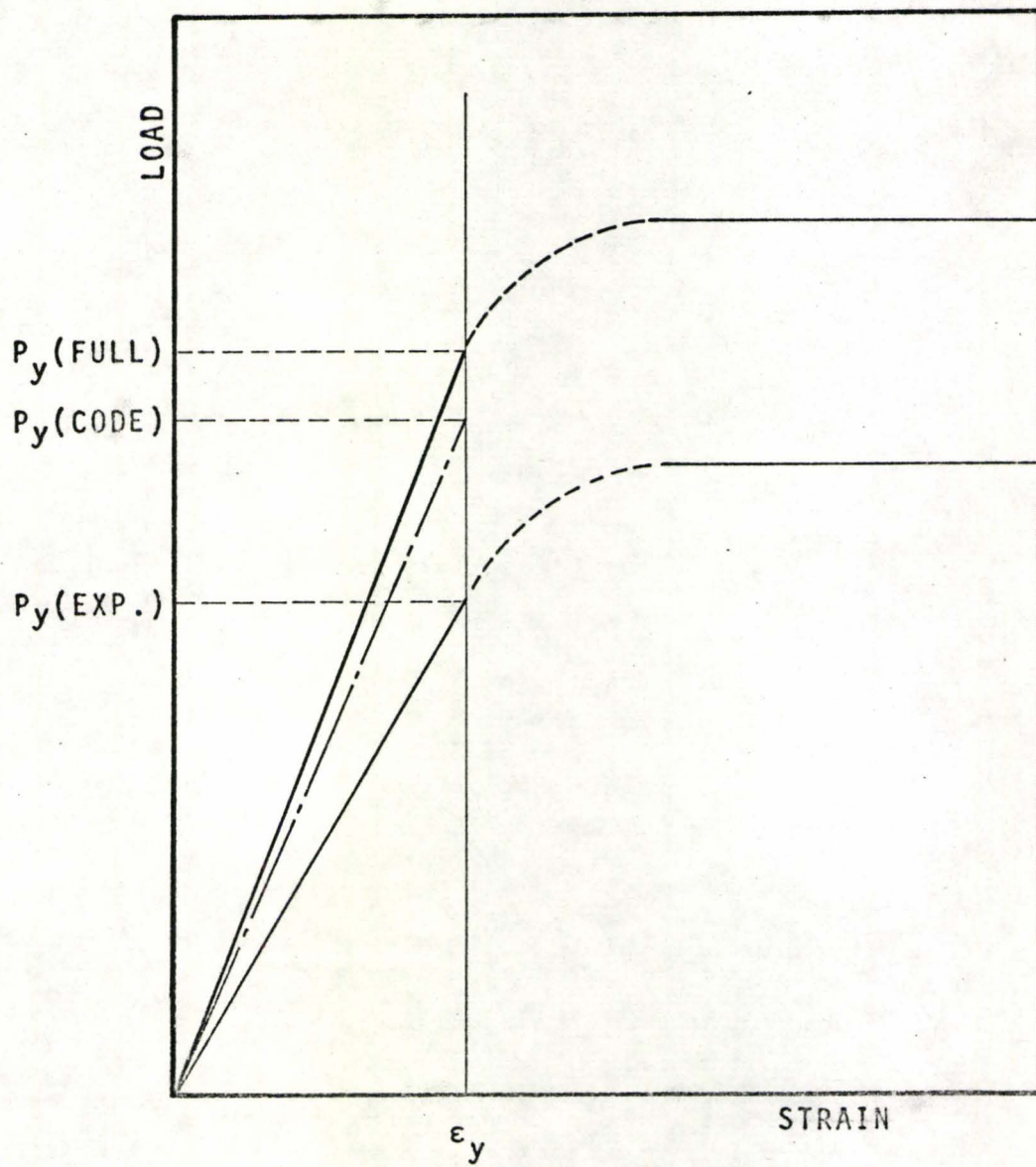


FIG. 5.2 LOAD FACTOR

CHAPTER VI

SUMMARY AND CONCLUSIONS

6.1 GENERAL

In the test beams intended to achieve full ultimate flexural capacity, Beams I and VI failed by fracture of the bottom chord and Beam IV failed by buckling of a web member.

All beams having partial connection failed by buckling of the top chord.

Two of the beams with partial connection had puddle welds (Beams II and IV), and these puddle welds ripped out of the metal decking prior to the buckling of the top chord.

In all test beams at working load the top chord stresses were never in excess of the allowable dead load stresses.

In general measured bottom fibre steel strains and deflections were larger than those predicted by the elastic analytical approaches.

The connector strengths calculated from ultimate moment considerations for the half inch stud, the single puddle weld and the double puddle weld were 6.50 kips, 2.10 kips and 5.36 kips respectively. The value from push-out tests was 5.5 kips for the half inch stud and for the double puddle weld.

An ultimate design method was derived which gave good agreement with the experimental results.

At a working stress of $0.60 F_y$, the beams with full connection had a load factor of at least 1.74 and the connectors in those beams had a load factor of at least 2.16.

It is recommended that a load factor of 1.7 could be used for the ultimate design method.

It is recommended that puddle welds may be used as shear connectors, in the case of their being the most economical, only for full composite action.

6.2 FUTURE RESEARCH

In further investigation of the use of puddle welds as connectors with this type of construction, the possibility of strengthening the metal deck around the welds by using washers or other means should be studied.

LIST OF REFERENCES

1. NEWMARK, N.M., SIESS, C.P. and VIEST, I.M., "Tests and Analysis of Composite Beams with Incomplete Interaction". Proceedings of the Society for Experimental Stress Analysis, Vol. IX, No. 1, 1951.
2. SLUTTER, R.G. and DRISCOLL, G.C., Jr., "Flexural Strength of Steel-Concrete Composite Beams". Journal of the Structural Division, ASCE, Vol. 91, No. ST2, Proc. Paper 4294, April 1965.
3. TIDE, R.H.R. and GALAMBOS, T.V., "Composite Open-Web Steel Joists". Research Report No. 4, Structural Division, Civil and Environmental Engineering Dept., Washington University, St. Louis, Mo., Feb. 1968.
4. NALL, M., HARMON, T., KONYALIAN, R. and GALAMBOS, T.V., "Experiments on Composite Open-Web Steel Joists". Research Report No. 13, Structural Division, Civil and Environmental Engineering Dept., Washington University, St. Louis, Mo., Jan. 1970.
5. ROBINSON, H., "Preliminary Investigation of a Composite Beam with Ribbed Slab Formed by Cellular Steel Decking". Engineering Dept., Report No. 35, McMaster University, October 1961.
6. ROBINSON, H., "Proposed Method of Establishing Design Criteria for Composite Steel and Concrete Beams Incorpora-

- ting Cellular Steel Decking". Dept. of Civil Engineering and Engineering Mechanics, McMaster University, Nov. 1964.
7. ROBINSON, H., "Tests on Composite Beams with Cellular Deck". Journal of the Structural Division, ASCE, Vol. 93, No. ST4, Proc. Paper 5391, Aug. 1967.
 8. ROBINSON, H., "Composite Beam Incorporating Cellular Steel Decking". Journal of the Structural Division, ASCE, Vol. 95, No. ST3, Proc. Paper 6447, March 1969.
 9. ROBINSON, H. and WALLACE, I.W., "Composite Beams with Partial Connection". ASCE Annual and National Environmental Engineering Meeting, St. Louis, Mo., Meeting Reprint 1549, Oct. 1971.
 10. CRAN, J.A., "Design and Testing Composite Open-Web Steel Joists". Draft Report, Sales Engineering Department, The Steel Company of Canada, Ltd., Hamilton, Ontario, 1971.
 11. Canadian Institute of Steel Construction, "Handbook of Steel Construction", Second Edition, Toronto, Ontario, Oct. 1970.
 12. American Institute of Steel Construction, Inc., "Manual of Steel Construction", Seventh Edition, New York, N.Y., 1970.
 13. A.C.I. Standard 318-71, "Building Code Requirements for Reinforced Concrete", American Concrete Institute, Detroit, Mich., 1971.
 14. ROBINSON, H., "Report on C.A.R.E.D. Project No. 141, Tests on Push-Out Specimens for The Steel Company of Canada,

Ltd.". Centre for Applied Research and Engineering Design
Inc., McMaster University, Hamilton, Ontario, Jan. 1970.